Journal of Thermal Analysis and Calorimetry (2023) 148:12369–12392
https://doi.org/10.1007/s10973-023-12544-z

A review of recent advancements in the crystallization fouling of heat exchangers

Kaleemullah Shaikh[1,2] · Kazi Md Salim Newaz[1,5] · Mohd Nashrul Mohd Zubir[1,6] · Kok Hoe Wong[3] · Wajahat Ahmed Khan[4] · Shekh Abdullah[1] · Md Shadab Alam[1] · Luvindran Sugumaran[1]

Received: 8 April 2023 / Accepted: 27 August 2023 / Published online: 14 October 2023

Abstract

A wide range of industrial processes (i.e., evaporation and condensation in desalination process, steam power plant, solar plant, etc.) involve heat transfer among the fluids. During the process of evaporative and cooling heat transfer, undesirable materials from the fluids accumulate on the surfaces, which critically reduces the performance of heat exchangers and creates one of the biggest challenges in energy transfer. Though the various studies on prediction and removal of fouling was conducted by numerous scientists, this problem is still unresolved in industrial process and is responsible for huge environmental damage and economic losses. This investigation provides a comprehensive overview of crystallization fouling in heat exchangers. Various factors affecting the deposition of crystallization foulaning such as fluid temperature, flow velocity, surface material and roughness, concentration and boiling are systematically reviewed. Accuracy and uncertainty of different equipment and experimental studies are discussed. In addition, fouling modelling is comprehensively discussed from earlier fundamental model to recent computational fluid dynamic and artificial neural networks model. Furthermore, mitigation of fouling with off-line and online approaches are chronologically discussed. Finally, an overview from environmental and economic prospective of fouling in heat exchangers are discussed. The future directions for crystallization fouling in heat exchangers are emphasized, which will support the researchers and industries to retard fouling and achieve economic benefits.

Keywords Heat exchanger · Fouling · Fouling mitigation · Fouling modelling · Environmental impacts · Economic evaluation

✉ Kazi Md Salim Newaz
salimnewaz@um.edu.my

✉ Mohd Nashrul Mohd Zubir
nashrul@um.edu.my

[1] Department of Mechanical Engineering, Faculty of Engineering, Universiti Malaya, 50603 Kuala Lumpur, Malaysia

[2] Faculty of Engineering, Balochistan University of Information Technology, Engineering, and Management Sciences (BUITEMS), 87100 Airport Road Quetta, Balochistan, Pakistan

[3] Carbon Neutrality Research Group (CNRG), University of Southampton Malaysia, 79100 Iskandar Puteri, Malaysia

[4] Nanotechnology and Catalysis Research Centre (NANOCAT), Institute for Advanced Studies, University of Malaya, 50603 Kuala Lumpur, Malaysia

[5] Centre of Advanced Manufacturing and Material Processing (AMMP), University of Malaya, 50603 Kuala Lumpur, Malaysia

[6] Centre for Energy Sciences (CES), University of Malaya, 50603 Kuala Lumpur, Malaysia

List of symbols

A	Surface area (m^2)
C	Concentration (gL^{-1})
D	Diffusion coefficient (m^2s^{-1})
ΔE_{12}^{TOT}	Total interaction energy (J)
h	Convection heat transfer coefficient ($Wm^{-2}\ K^{-1}$)
K_m	Fluid deposit mass transfer coefficient (ms^{-1})
K_r	Rate of reaction ($m^4kg^{-1}\ s^{-1}$)
K_s'	Deposit solubility product
m	Mass (kg)
$\dot{m}$	Mass flow rate ($kg\ s^{-1}$)
n	Order of reaction
Q	Heat (J)
R	Thermal resistance (m^2KW^{-1})
Ra	Arithmetic mean aberration
Re	Reynold number
Rz	Average surface roughness depth (μm)
Sh	Sherwood number
t	Time (s)
T	Temperature (K, °C)

U	Overall heat transfers coefficient (Wm^{-2} K^{-1})
v	Velocity (ms^{-1})
Wa^*	Work of adhesion
x	Thickness (m)

Greek symbols

λ	Thermal Conductivity, Wm K^{-1}
β	Inverse of time constant, s^{-1}
τ	Shear stress, Nm^{-2}
ρ	Density, kg m^{-3}

Subscription and superscription

*	Asymptotic
b	Bulk solution
c	Clean
d	Deposit
f	Fouling
r	Removal
sat	Saturation

Abbreviations

ANN	Artificial neural network
AEMF	Altering electromagnetic field
ANNM	Artificial neural network model
CFD	Computational fluid dynamic
DTPA	Diethylene triamine pentaacetate
EAF	Electronic antifouling
EDM	Electric discharge machining
EDTA	Ethylenediaminetetraacetic acid
FFNN	Feed-forward neural network
GDP	Gross domestic product
GNP	Gross national product
MWCNT	Multi-walled carbon nanotubes
PTFE	Polytetrafluoroethylene
SCMC	Sodium carboxymethyl cellulose
SEM	Scanning electron microscopy
SWRO	Sea water reverse osmosis
US	Ultrasonic
USD	United States dollar
VG	Vortex generator
XRD	X-ray diffraction

Introduction

Fouling or formation of mineral scale is a process where undesired dissolved minerals (dissolved in the cooling fluid) are deposited on the surfaces of the heat exchangers [1]. It is a common problem in desalination plants, water heat exchangers [2], process plants, steam producing units and household equipment [3]. Fouling in heat exchangers is a problem as it enhances pressure drop and creates extra hurdles in heat transmission, and encourages tube material corrosion. These influences can gradually decrease the efficiency of heat transfer, and after a certain time, it loses its acceptable efficiency limit and imposes forced shutdown, and finally, it reduces operating service life of the heat exchangers. Thus, fouling is considered as a critical constraint in operation and design of heat transfer equipment [4].

The fouling effect on heat transfer equipment is commonly explained through the additional thermal resistance owing to fouling layer. Thus, the overall heat transfer coefficient (U) of the fouled equipment is calculated by using Eq. 1 [5].

$$\frac{1}{U} = \left(\frac{1}{h_1} + R_{f,1}\right)\frac{A_2}{A_1} + R_{Wall} + \frac{1}{h_2} + R_{f,2} \tag{1}$$

where A and h are the heat transfer area and the heat transfer coefficient, respectively, of the heat transfer fluids. R_{wall} is the thermal resistance of the wall separating the two heat transfer fluids. R_f is the fouling resistance developed by the crystals deposits, depending on the situations of the heat exchanger, where the crystals can deposit on one or both the sides of the wall as shown in Fig. 1. The term R_f can be defined as the difference between the inverse values of the overall heat transfer coefficient before the fouling (U_o) and after the fouling (U_f) occurred as shown in Eq. (2):

$$R_f = \frac{1}{U_f} - \frac{1}{U_o} \tag{2}$$

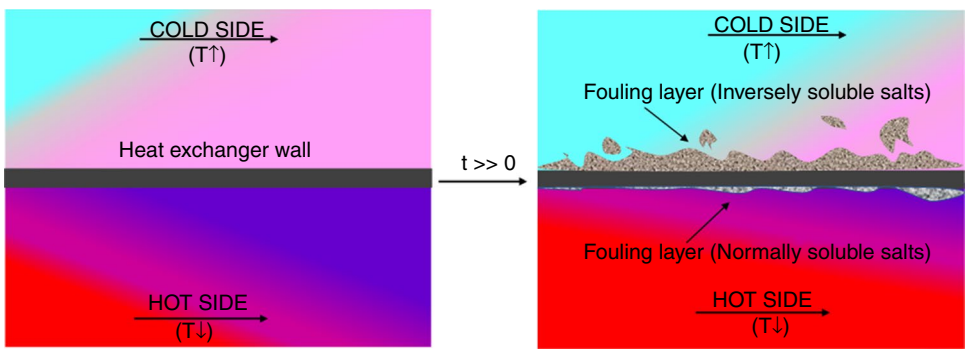

Fig. 1 Schematic of fouling on heat exchanger [5]

If the value of U assumes constant throughout the area of heat exchanger, the additional heat transfer surface area is desired to attain the same performance as stated by Eq. (3).

$$A_f = A_o\left(1 + R_f \cdot U_o\right) \tag{3}$$

Likewise, if the heat exchanger area assumed constant, enhancement in temperature difference among the hot and cold water stream is required to maintain the similar performance of the heat exchanger (Eq. 4).

$$\Delta T_f = \Delta T_o\left(1 + R_f \cdot U_o\right) = \Delta T_o \frac{U_o}{U_f} \tag{4}$$

If the parameters shown in Eqs. 3 and 4 have not accommodated the adjustment of the fouling, then the decline in performance of heat exchanger will appear and it could be presented by Eq. 5.

$$Q_f = \frac{Q_o}{1 + R_f \cdot U_o} \tag{5}$$

According to Bott [6], fouling can be categorized in six types such as (i) crystallization fouling, (ii) corrosion fouling, (iii) particulate fouling, (iv) chemical fouling, (v) solidification fouling and (vi) biofouling; among these six types of fouling, crystallization fouling is responsible for more than 25% of problems faced due to the fouling. Crystallization fouling on heat transfer surfaces is commonly occurred due to the accumulation of salts from insolubility, which occurred from the degree of enhanced supersaturation, and augmented temperature. It is reported that the process of crystallization fouling phenomena can be separated into three phases as shown in Fig. 2, i.e., (i) induction phase, (ii) roughness control phase and (iii) deposit growth phase. In the induction period, stable nuclei formation and growth of crystal appear on the heat transfer surface, while in roughness control period the fouling resistance decreases because of the expansion in surface area comparative to smooth surface [7, 8], whereas fouling growth period enhances the fouling resistance against time owing to the formation of dense fouling layer. Crystallization fouling process associates with several fields, i.e., chemical kinetics, heat and mass transfer, material science and so on [9].

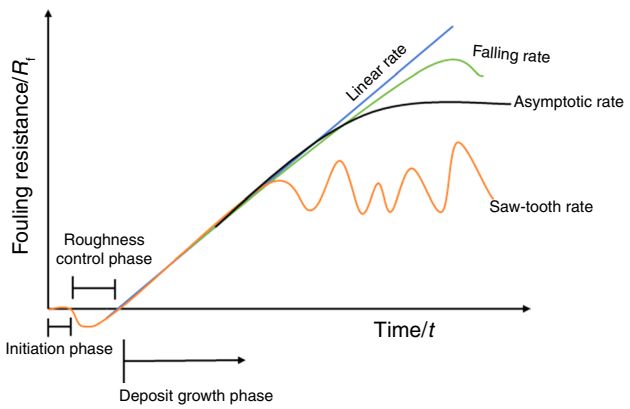

Fig. 2 Different fouling phases and usual types of curves

Several scientists and industrialists from various field have been challenged for this fouling issues. They observed difficulties and complexities in fouling area [10–12]. The purpose of this study is to provide the comprehensive overview of the recent advancement of the crystallization fouling in heat exchangers and steps involving in this study are mentioned in the flowchart shown in Fig. 3. For this purpose, the authors conducted this review with an overall introduction of fouling and formation of crystals on the heat exchanger surfaces. Different fouling phase and process were comprehensively studied. Effects of numerous parameters on fouling rate are elaborated from the crystallization point of view; various effectual cleaning and mitigation strategies for the reduction of fouling were systematically studied. Uncertainty and accuracy of equipment used in different fouling rigs were discussed. Fundamental model to recent CFD and neural network model were explored, and finally, the impact of fouling on environment and economic was reviewed. Efforts were also made for some new interest in this field, and some possible new research directions were elaborated. This study will provide the benefits to the industrial stake holders to enhance the efficiency of the heat exchangers utilized in different industrial process applications and EPA to control the emissions of the hazardous gasses.

Crystallization fouling

For experimental investigation, supersaturated inverse soluble mineral salts solutions were prepared by the researchers to accelerate the deposition on heat exchanger surfaces for the study of their deposition, formation, mechanism and mitigation.

Through dissolving the mixture of calcium nitrate tetrahydrate ($Ca(NO_3)_2{\cdot}4H_2O$) and sodium sulphate ($NaSO_4$) powders in distilled water, artificial hard water of $CaSO_4$ was synthesized to perform the experiments. Equation (6) shows the $CaSO_4$ formation reaction [13, 14].

$$Ca(NO_3)_2 \cdot 4H_2O + Na_2SO_4 \rightarrow CaSO_4 \cdot 2H_2O + 2NaNO_3 + 2H_2O \tag{6}$$

Likewise, $CaCO_3$ solution was synthesized through the reaction of dissolving calcium chloride ($CaCl_2$) and sodium bicarbonate ($NaHCO_3$) in stochiometric ratios, and Eq. (7) shows the reaction and formation of $CaCO_3$ solution [13, 15].

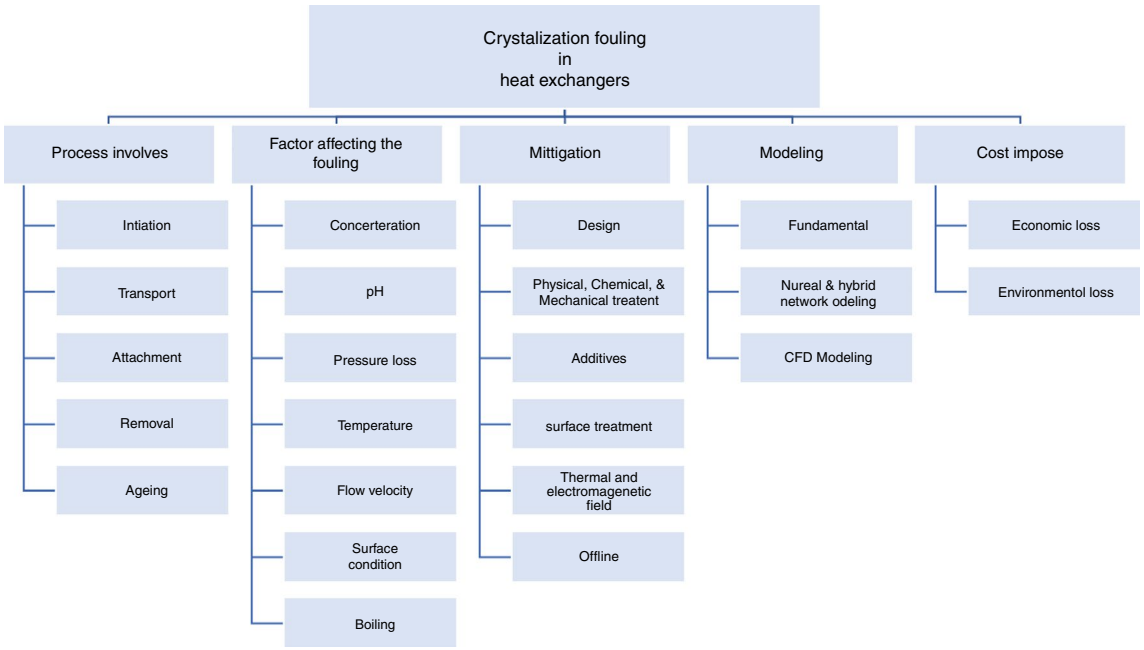

Fig. 3 Flowchart of current study

$$CaCl_2 + 2NaHCO_3 \rightarrow CaCO_3 + 2NaCl + H_2O + CO_2 \quad (7)$$

Similarly, for hard water solution of $CaSO_4$ and $CaCO_3$ composite, $CaSO_4$ was prepared with the same reaction as mentioned in Eq. 6 while for perpetration of $CaCO_3$, calcium chloride ($CaCl_2{\cdot}2H_2O$) and sodium bicarbonate ($NaHCO_3$) were dissolved to perform the reaction and produce the solution of $CaCO_3$ as shown in Eq. 8. After synthesizing $CaSO_4$ and $CaCO_3$, stoichiometric ratio of $CaSO_4$ and $CaCO_3$ solution was used for performing the experiments [16].

$$CaCl_2 \cdot 2H_2O + 2NaHCO_3 \rightarrow CaCO_3 + 2NaCl + 4H_2O + CO_2 \quad (8)$$

In the industries, high concentration of organic phosphate in cooling tower is utilized to reduce the corrosion, and river and lake water also accumulated organic phosphate from agricultural runoff. This organic phosphate can easily be oxidized with discrete oxidizers such as chlorine present in the cooling water which reacts with the organic phosphate and produces orthophosphate ion which gives rise to $CaPO_4$ fouling on the surface of heat exchangers [17].

The impact of foulants removal and deposition on heat exchanger surface was significantly noticed in the fouling as shown in Fig. 1. The fouling process in terms of foulant deposition and removal can be presented through Eq. 9 as given by Kren and Seaton [18].

$$\frac{dm_f}{dt} = \dot{m}_f = \dot{m}_d - \dot{m}_r \quad (9)$$

where $\dot{m}_f$, $\dot{m}_d$ and $\dot{m}_r$ are the net deposition rate, deposition rate, and removal rate, respectively. For the typical fouling system, numerous removal (i.e., erosion, dissolution and spalling) and multiple depositions (such as sedimentation and crystallization) were predicted by researchers [19].

Both removal and deposition process occur simultaneously, and it depends on various operating conditions such as surface roughness, flow velocity and operating temperature. At the interface of fouling, the reduction in the temperature is noticed with the raise in deposits, that decline the temperature further reduces the rate of deposition and produces a steady-state slope [19].

Mathematical, foulant mass deposition rate per unit area ($\dot{m}_f$) in terms of fouling factor (R_f), foulant density (ρ_f), thickness of deposit layer (x_f) and thermal conductivity of foulant (λ_f) can be expressed using Eq. (10).

$$\dot{m}_f = \rho_f x_f = \rho_f \lambda_f R_f \quad (10)$$

Crystallization fouling process

Fouling is a complicated phenomenon because of the involvement of several numbers of variables. In terms of the fundamentals, the fouling phenomena follow several processes in growing deposition on the surface. Epstein [20] divided fouling phenomena into five different categories based on the most common fouling mechanisms: crystallization fouling, particulate fouling, corrosion fouling, chemical

fouling and biofouling as shown in Fig. 4. Here, the light highlighted sections represent that the scientists have average understanding about the process in all the five fouling mechanisms while the dark highlighted sections demonstrate that the researchers have good or excellent understanding about the processes in all the five fouling mechanisms, whereas no highlighted sections represent that the researchers have poor understanding about the processes. The main fouling process was subdivided into different stages such as initiation, transport, deposition, removal and ageing [21, 22]. In this study, these five stages were discussed based on crystallization fouling because the present study is focused on review of crystallization fouling.

Initiation

The surfaces are conditioned during the initial period. At the beginning of the fouling experiment, the induction period was affected by the surface material, surface temperature, coatings and surface roughness. Due to the increase in the surface temperature and degree of supersaturation, induction period decreases. With the deposit formation, the crystallization nuclei appear in the induction period. This period can last from few seconds to numerous weeks depending on the chemical concentration, surface temperature, roughness, fluid flow velocity, etc. The crystallization fouling could be changed because of the decrease in induction period due to the rise in the surface temperature [20]. The induction period tends to reduce with the rise in roughness of surface. Moreover, crystallization fouling is encouraged due to the sites established by roughness on surface [21].

Fouling matrix		Fouling mechanism				
		Crystallization	Particulate	Chemical	Corrosion	Biological
Fouling process	Initiation					
	Transport					
	Deposition					
	Removal					
	Aging					

Fig. 4 Epstein 5×5 matrix to characterize the fouling process, light to dark shading present enhanced in level of understanding [20]

Transport

In transport, fouling substances in bulk fluid are transited towards the heat exchanger surface through the boundary layer as shown in Fig. 5f. It depends on concentration difference among the bulk solution and surface fluid boundary layer [22]. The foulants transport to the surface is usually based on diffusion and convective mass transfer film theory, and the mechanisms would be different for suspended particulates and crystallize foulants [25]. The surface deposition flux can be expressed by Eq. (11).

$$m_d = h_d\left(C_b - C_s\right) \tag{11}$$

where m_d is mass transfer convection coefficient, and C_b and C_s are bulk solution concentration and concentration nearer the surface of heat transfer, respectively. h_d can be found from Sherwood number ($Sh = h_d/d$) which depends on geometric and flow parameters.

Attachment

Once foulant transported, deposits stick with each other or with the surface or they leave the surface to adhere at any other place. Factors which can affect the adhesion are surface shear force, surface energy, surface temperature and composition of earlier deposited layer. Due to the electromagnetic forces, the salt ions arrive at the surface and adhere to the surface for forming the nuclei. The formed nuclei slowly raise with time and form fouling layer. So, for the determination of attachment, forces acting on salt ion are important as they approach to the surfaces. Properties of deposits and surface (i.e., surface situation, size and density) are the dominant phenomena of the attachment of deposits [20, 21, 25].

Removal

Initially, in comparison with the deposition mechanism, the removal mechanisms were poorly understood [18]; later

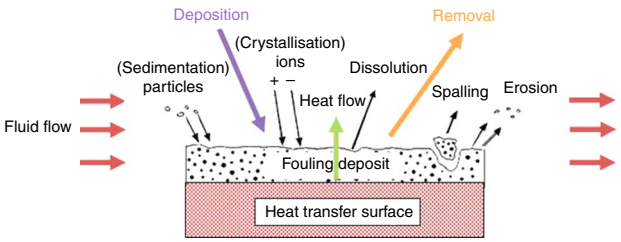

Fig. 5 Deposition and removal of crystallize foulant on heat exchanger surface [26]

scientists comprehended that the shear force among the fluids and foulant deposition were responsible for removal of foulants due to involvement of numerous factor such as velocity gradient at surfaces, surface roughness and viscosity of fluid. The fouling model commonly assumes that the net deposition rate is the difference between the deposition rate and the removal rate as shown in Eq. (9). Based on Kern and Seaton model, the fouling curve can behave like four different forms as per the removal rate such as linear, falling, asymptotic and sawtooth as shown in Fig. 2 [5, 13, 27, 28]. If the removal rate is constant or negligible, then the linear fouling curve is obtained, and when the removal rate is variable, sawtooth curve is formed. Similarly falling curve is obtained from higher removal rate, whereas asymptotic fouling is developed when the removal rate is equal to the deposition rate. Shear forces at boundary between the fouling deposit and fluid are accountable for removal. Shear forces are determined through surface velocity gradient, surface roughness and fluid viscosity. Surface removal is performed by mechanism of erosion, spalling and dissolution as shown in Fig. 5 [21].

Ageing

Ageing of foulant deposits starts soon after the accumulation on heat transfer surface [20]. Ageing quantitative data are rarely reported because many fouling deposits required large time scale to age [29, 30]. The process of ageing may include the change in chemical structure or crystal, i.e., polymerization or dehydration [21, 25]. These changes particularly at constant heat flux increase the temperature of deposits and strengthen the foulant deposits with time. These alterations during the ageing also change mechanical properties of deposits. Mechanical strength of foulants can be altered through the change in chemical composition of foulants by chemical reaction [21].

Factors affecting the crystallization fouling rate

Fouling depends on numerous factors such as type of mineral and its composition present in bulk solution, flow velocity, pressure loss, temperature, pH, boiling and surface condition. These parameters are broadly explained below in detail:

Solution concentration

Fouling deposition expedites with the increase in the concentration of foulants in the solution. Figure 6a depicts that the deposition rate of $CaSO_4$ at 3.6 g L^{-1} concentration is much higher than the deposition rate of $CaSO_4$ at 3.0 g L^{-1},

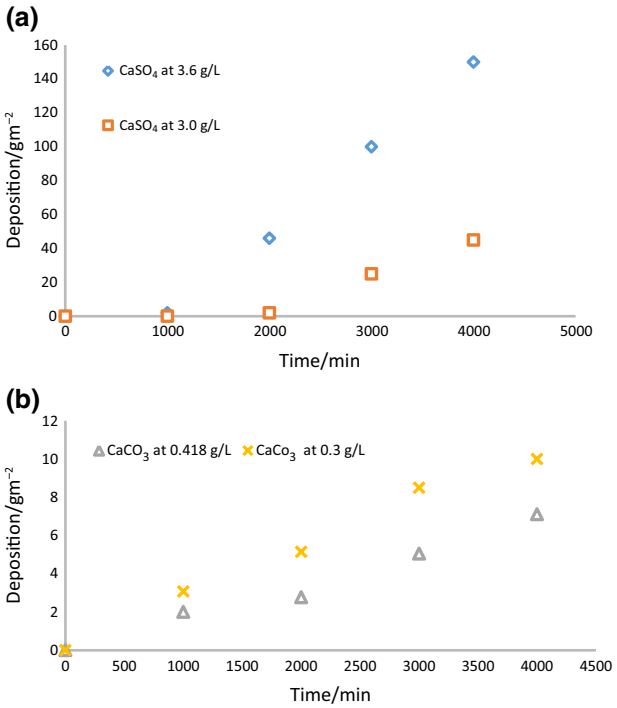

Fig. 6 **a** Deposition of $CaSO_4$ at two different supersaturated concentration [29]. **b** Deposition of $CaCO_3$ at two different supersaturated concentration [28, 30]

similarly, Fig. 6b reveals that deposition rate of $CaCO_3$ at 0.418 g L^{-1} is greater than that at the 0.30 g L^{-1} of $CaCO_3$ concentration. Researchers also conducted the studies on influence of fouling composition on heat exchanger surface [31]. They examined the normal soluble salts ($NaSO_4$ and NaCl) characteristics as composite crystallization fouling in double-pipe heat exchangers. Due to the common ion influence, $NaSO_4$ is mainly deposited on heat transfer surface.

NaCl significantly influences the supersaturation of $NaSO_4$, while the increase in mass percentage of NaCl in mixture solution gradually reduced the fouling thermal resistance and prolonged the asymptotic thermal resistance. Choi et al. [32] examined the $CaSO_4$ crystallization fouling in seawater reverse osmosis (SWRO) desalination and observed similar influence of NaCl. The existence of NaCl reduced the growth of $CaSO_4$ crystals and permitted the formation of larger crystals. Helalizadeh et al. [1] investigated the effect of composite salts on crystallization fouling. Linear increase in fouling was noticed with the enhancement of thermal resistance in the presence of mixture concentration of $CaSO_4$ and $CaCO_3$ at 2 g L^{-1} and 1 g L^{-1}, respectively, while at 1 g L^{-1} and 0.4 g L^{-1} composition, a very little variation in fouling and thermal resistance was observed. Chong and Sheikholelami [33] investigated the mixed crystallization fouling of $CaCO_3$ and $CaSO_4$ and found that the addition of $CaSO_4$ reduced the $CaCO_3$ deposit strength. Due to

its stronger adherence, various research groups observed that $CaCO_3$ had a stronger effect on fouling than $CaSO_4$. When both the compounds were dissolved in water simultaneously, the deposit properties approximated to $CaCO_3$. Song et al. [16] conduct a study on $CaSO_4$ and $CaCO_3$ mix fouling characteristics on plate heat exchanger surface. Results of this study support the investigation [34] on composite scale formation of $CaSO_4$ and $CaCO_3$ that reveals the precipitation of particles behaved as additional nucleation spots that speed up the rate of deposition and increased fouling [34]. However, $CaCO_3$ becomes less adherent and $CaCO_3$ solubility increased with the addition of $CaSO_4$ [1]. This study also observed that in comparison with $CaCO_3$ fouling, composite fouling of $CaCO_3$ and $CaSO_4$ produced a longer asymptotic fouling period due to the increase in solubility of composite fouling that cause greater average precipitation on higher temperature than $CaCO_3$ fouling alone. Furthermore, the deposition rate produced by $CaCO_3$ fouling is higher than the composite fouling owing to the higher adhesion of $CaCO_3$ than the combined fouling. Moreover, the relation between concentration of $CaCO_3$ and asymptotic fouling period is inversed when the concentration of $CaCO_3$ increased, the asymptotic fouling period decreased [16]. Similarly, Kromer et al., 2015, [35] investigated the mixed salt formation and its mitigation of fouling in seawater falling tube evaporation desalination equipment. Study indicated that $Mg(OH)_2$ developed a layer on surface of copper–nikel in the form of brucite. Even at a low evaporation temperature, i.e., 50 °C, magnesium-rich scale was formed which supported the assumption of the study that the high pH value at the solution–metal interface. Researchers also found that once the surface was fully covered with magnesium then the growth of magnesium layer stopped and precipitation of $CaCO_3$ in aragonite form started. They also found an inverse relationship between the Mg^{2+} and $CaCO_3$, which means that with the increase of Mg^{2+}, the $CaCO_3$ concentration was decreased.

pH

In crystallization fouling, pH plays an important role and effect of pH on fouling is not straightforward [4]. Researchers studied the effect of pH on the deposition of crystallize foulant on heat exchangers surface. Höfling et al. [39] studied the impact of pH on $CaCO_3$ and $CaSO_4$ composite fouling deposition.

This depicts that at $pH < 6$ only $CaSO_4{\cdot}2H_2O$ was accumulated on the surface of heat exchanger, while at pH 7.0 $CaSO_4{\cdot}2H_2O$ and $CaCO_3$ (in aragonite and calcite form) were deposited, whereas at pH 7.5 $CaSO_4{\cdot}2H_2O$ and $CaCO_3$ (in aragonite form) and at 9.0 pH value $CaSO_4{\cdot}2H_2O$ and $CaCO_3$ (in vaterite form) were detected in X-ray diffraction. Constant $CaSO_4$ saturation at pH value between 4.0 and 10 was found as shown in Fig. 7. Some researchers [1, 4] reviewed the effect of pH on fouling deposition. Reduction in fouling precipitation was found with the increase in the pH value. For the consideration of polymorphism of $CaCO_3$, pH was most important factor. When $10 \leq pH \geq 12$, it enhanced the aragonite formation. At $pH < 11$ and low temperature (about 7 °C), mostly pure calcite was formed, whereas pure aragonite was formed at 58 °C for $pH < 10$. However, $CaSO_4$ is not significantly affected by pH and tends to precipitate in various forms once the solution becomes supersaturated. Augustin and Bohnet [40] studied the influence of pH on $CaCO_3$ fouling. To resist the corrosion, most of the heat exchangers required $pH > 6.0$ and fouling resistance of $CaCO_3$ is also increased above the 6.0 pH value. The asymptotic fouling resistance increases with the pH values due to a higher strength of the fouling layer caused by an increasing crystal growth velocity for supersaturation. Similar study for $CaSO_4$ depicts fouling behaviour change below 4.0 pH value.

Pressure loss

The quantification and detection of fouling mechanisms in different industries depend on two crucial parameters: (1) the pressure drop Δp and (2) the fouling resistance R_f [41] as shown in Fig. 7. The first parameter illustrates the rise in the pressure loss owing to the changing in surface roughness and a decline in cross-sectional area. Therefore, the pressure drop directly relates to the deposited mass which blocks the flow passage. Figure 8 shows that the time-related fouling can be divided into various phases. During the early initiation stage, the surface was preconditioned, and no notable variation in pressure drop or thermal resistance was evidenced. In the succeeding roughness-controlled stages, the deposits began to form on the surface and raised the pressure loss due to the higher roughness, and enhanced the heat transfer [7]. Both stages together can be called as an

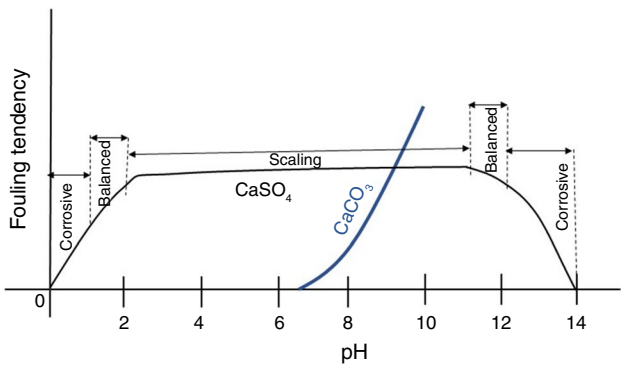

Fig. 7 pH effects on $CaSO_4$ and $CaCO_3$ fouling [39, 40]

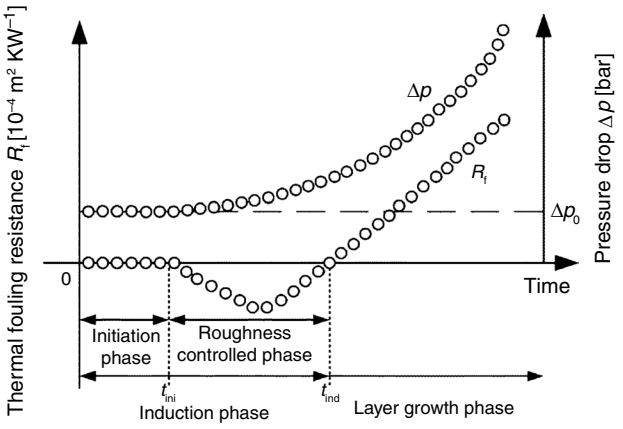

Fig. 8 Schematic formation of thermal resistance and pressure drop with respect to time [41, 42]

induction stage. After induction stage, the layer growth stage starts in which the deposits continuously develop on the surface of heat exchanger, which raises the pressure loss, and enhances the thermal resistance of heat exchanger. The second parameter, the thermal resistance was earlier explained in the introduction section.

Temperature

One of the most important parameters influencing the fouling is temperature, i.e., bulk and surface temperature. The salt's (such as $CaCO_3$ and $CaSO_4$) solubility shows an inverse solubility characteristic with temperature, i.e., solubility decreases with the increase in the temperature. Hence, on heated surfaces, these salts tend to crystalize and deposit, and additionally heterogeneous nucleation mechanisms are also supporting salts deposition. In aqueous supersaturated solutions, $CaCO_3$ is formed in polymorphs and strongly influenced by the temperature [31]. Though the solubility of calcite is less, but the calcite is the most thermodynamically stable form of $CaCO_3$ and vaterite is the least stable form of $CaCO_3$ [43]. Calcite has hexagonal crystal form and commonly formed at room temperature. Aragonite is belonging to orthorhombic system and does not change to calcite when heated in dry air and 400 °C. Conversion rate of $CaCO_3$ is increased with the increase in the temperature; when $CaCO_3$ contacted with aragonite, conversion can take place at room temperature. Wang et al. [44] observed an opposite transformation trend. In the existence of surface Zinc composite coating, $CaCO_3$ fouling morphologies changed from calcite to aragonite.

Due to least solubility, anhydrite is the most stable crystal form of $CaSO_4$ when higher temperature is considered. However, nucleation process of anhydrite is slow [45]; therefore, crystals of gypsum are normally formed. Gypsum in both the cases, before dehydration and after rehydration, is commonly precipitated in the range of 40–98 °C, where hemihydrate and anhydrite species are possible. Inversely soluble salts are frequently noticed in scaling investigation, where it demonstrates the enhanced deposition rate with the higher inlet temperature of heat exchangers as shown in Fig. 9.

Figure 8 demonstrates the results of studies conducted by different researchers on effect of surface temperature on fouling resistance, in which study conducted by Dong et al. [46] shows that at 2.3 gL^{-1} $CaSO_4$ concentration, fouling resistance increased with the enhance of surface temperature. At 3.4 gL^{-1}, $CaSO_4$ concentration initially increased with the rise of surface temperature, but after 75 °C fouling becomes asymptotic. Similarly, study conducted by Atika et al. [47] shows at 0.4 gL^{-1} concentration of $CaCO_3$ fouling resistance rise with the enhance in surface temperature.

Flow velocity

The flow velocity has strong impact on fouling rate. Due to the hydrodynamic effects such as surface shear and eddies stress, flow velocity has direct impact on both removal

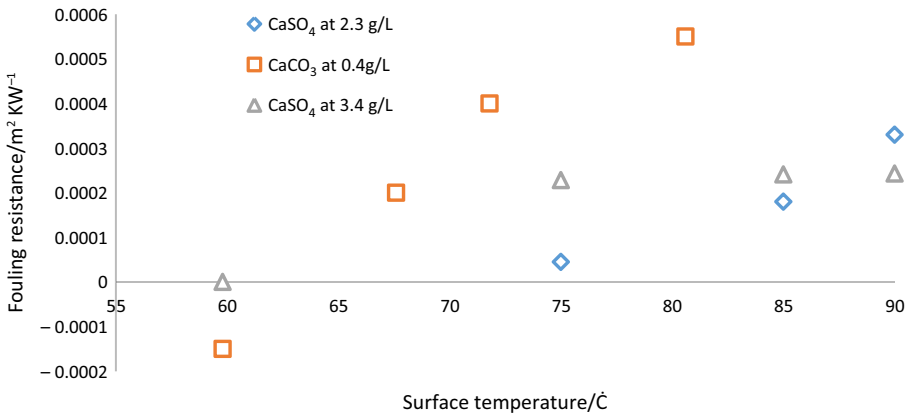

Fig. 9 Fouling resistance at different surface temperatures [46, 47]

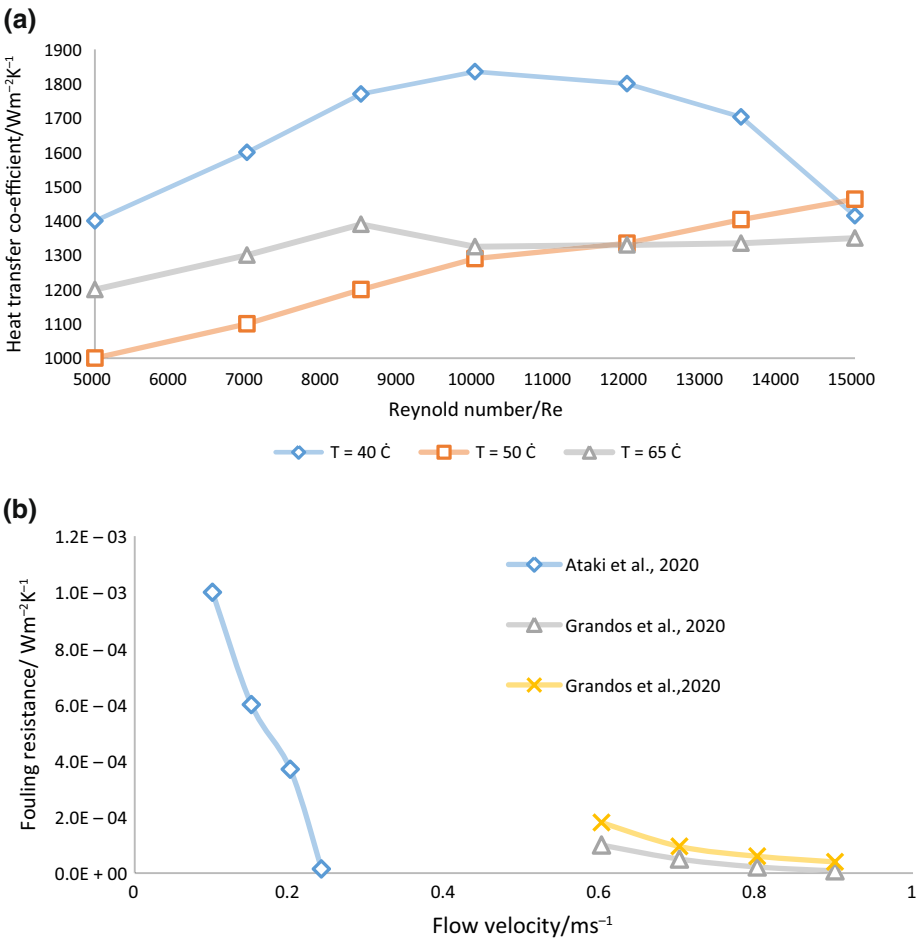

Fig. 10 Effect of flow velocity on **a** the overall heat transfer coefficient [15], **b** fouling resistance [9, 36, 47] as a function of flow velocity

and deposition rate. In contrast, it has indirect impacts on the mass transfer coefficient, sticking ability and deposition strength. During the force convection heat transfer, many studies on scale formation have been performed [4]. Results of these studies show that high velocity sometimes accelerates the fouling [48] while in some cases it reduces the deposition [49]. According to the study conducted by Helalizadeh et al. [1], the fouling mechanism is clearly diffusion-controlled at lower fluid velocity. However, fouling process changed to reaction controlled at increasing flow velocity. If the mass transfer in the fouling process is not controlled, then the deposition rate remains independent of flow velocity if surface temperature stays constant.

Figure 10a strengthens the statement of Hatch [48] that higher flow velocity reduces the overall heat transfer coefficient, while Fig. 10b demonstrates that with the increase in the flow velocity the fouling resistance reduces [9, 36, 47], which supports the statement of Zhao and Chen [4] that fouling can directly affect the removal rate.

Surface condition

In recent years, surface material and its morphology has enhanced the interest of researchers and is considered as one of the important influencers in crystallization fouling. Teng et al. [50] characterized the behaviour of various surface materials for the study of $CaCO_3$ crystallization fouling using double-pipe heat exchanger. The results illustrated the linear growth relationship among the rising thermal conductivity of studied surface and foulant deposition. This investigation also supports the studies conducted by other researchers, i.e., Wang et al., [51] and Cooper et al., [52], where descending order of foulant deposits were observed i.e., copper > aluminium > stainless steel. Wang and Yang [53] observed that silicon carbide (SiC) surface coating reduced the fouling deposition by 4 times than that on stainless steel surface. If surface material used is also prone to corrosion, then the enhanced fouling can be observed [53]. This fouling effect can be critically reduced through the developing of oxide thin layers on the metal surfaces that obstruct the additional corrosion. Similar to corrosion, occurrence of organic layer also acts

as an accelerator of fouling layer [55]. Cooper et al., [56] revealed that fouling resistance in plate heat exchangers significantly reduced due to turbulence produced through the plate corrugation. Han et al. and Xu et al. [57, 58] observed from numerical model that shorter distance between the vortex generators (VGs) produces larger turbulence. When the distance between VGs exceeds 55 mm, the characteristics found were similar to non-VGS. Hasan et al. [59] found that asymptotic fouling resistance was brutally decreased due to the use of multiple turbulence generators on the surface of heat exchanger, which indicates great potential in getting the trade-off benefit among the fouling mitigation, pressure drop through VGs and improvement in heat transfer[60]. Hasan et al. [61] also examined the fouling properties impact due to the mechanical increment in surface for the attainment of higher heat transfer rate. In double-pipe heat exchanger, coil wire was used, which enhanced the turbulence near the surface, and crucially obstructed the fouling and boosted the heat transfer. Examination of $CaSO_4$ fouling conditions on shot-peened surfaces validated the observations of AL Janabi and Malayeri [62]. In the presence of the shot peening surface, the roughness enhanced, induction period reduced, and initial fouling rate improved considerably. Furthermore, short, peened surface deposits were resilient, thicker and more equally structured. Under the fouling condition, porous surfaces were also examined. Großerichter and Stichlmair, and Zhao et al. [63, 64] investigation concluded that these shot peening surfaces should not be utilized in applications where intense fouling is expected owing to the accumulation of severe deposits.

Roughness is a degree of the surface texture and can be calculated through the vertical aberrations of real surface to its ideal state. Surface roughness is generally defined by numerous parameters, i.e., *R*z (the average roughness depth) and *R*a (the arithmetic mean aberration) [65]. Heat transfer effects due to surface roughness are well recognized and are broadly used to enhance the various heating equipment performance [3, 66, 67]. Two effects, which may contribute in enhancement of heat transfer owing to roughness, are (i) enhancement in turbulence near the wall and (ii) an addition of surface area comparative to smooth wall [7]. Lei et al.,[70] recognized that surface texture has very strong impact on size, distribution and growth rate of $CaCO_3$ crystal accompanied by enhancing the fouling rate. Yoon and Lund [71] stated that surface roughness effect was not found at Ra 0.08–0.60 µm.

McGuire and Swartzel [72] demonstrate that surfaces with Ra values of 0.41, 0.04, 1.93 and 2.31 µm for rough, polish stainless steel, aluminosilicate and polytetrafluoroethylene (PTFE) coating, respectively, were not a factor for fouling. Malayeri and Müller-steinhagen [73] also recognized that deposition of $CaSO_4$ was severely affected through the surface roughness level, and on rough surface, higher fouling layer was found; hence, higher roughness induced shorter induction periods.

Boiling/bubble formation

Crystallization fouling is more critical if boiling occur due to bubbles formation process. The presence of bubbles reduces the resistance of boundary layer, which makes easier for salts to stick on heating surface [5, 74]. Moreover, bubbles formed in boiling enhances shear stress due to the rise in turbulence near the surface that leads to reduction in fouling rate through suppression or removal [74]. Sometime fouling process itself is a cause to transit in nucleate boiling due to the surface temperature rises because of deposits formed as indicated by Elhady and Malayeri [75]. They investigated $CaSO_4$ crystallization fouling impacts and perform numerous experiments at constant heat flux circumstances and illustrated enhance in surface temperature more than boiling point due to the fouling leads bubbles nucleation. They also found boiling occur after the induction period, where crystallization fouling mechanism transfer from convective heat transfer to subcooled boiling. Malayeri et al. and Rashidi et al. [76, 77] reported that bottom pipe deposits in bundle are usually dense and adherent. The enhancement in bubble formation has tendency to increase the bundle shear force and heat transfer rate on pipe surfaces and both reduced the deposition rate. Haghshenasfard et al. [78] created a mathematical model for the prediction of $CaSO_4$ fouling under the subcooled boiling. They observed from the results that surface temperature is enhanced with the increase in the deposition rate. Due to the rise in the fluid velocity, deposition rate decreases and resistance in fouling is enhanced. Peyghambarzadeh et al. [79] assessed the capabilities of asymptotic model for the prediction of $CaSO_4$ fouling during the subcooled boiling. To predict the fouling occurrences under the boiling circumstances, model has simplicity and high accuracy; for the nucleate boiling fraction, model has significant prediction capability. Nucleate boiling fraction is a vital factor in fouling process under boiling situations compared to other models. For example, Chen et al. [80] developed model for the prediction of fouling during the subcooled boiling but model cannot estimate nucleate boiling fraction with high precision.

Figure 11a demonstrates the transport mechanism and development of microlayer on the surface of heat exchanger. It is clearly predicted from the figure that during the bubble growth, $CaSO_4$ ions in microlayer remain trapped and water evaporation causes it to become intensively supersaturated. Figure 11b shows the images of bubble departure as a function of heat flux at constant concentration of $CaSO_4$ which shows the direct relation between heat flux and thickness of scale deposits.

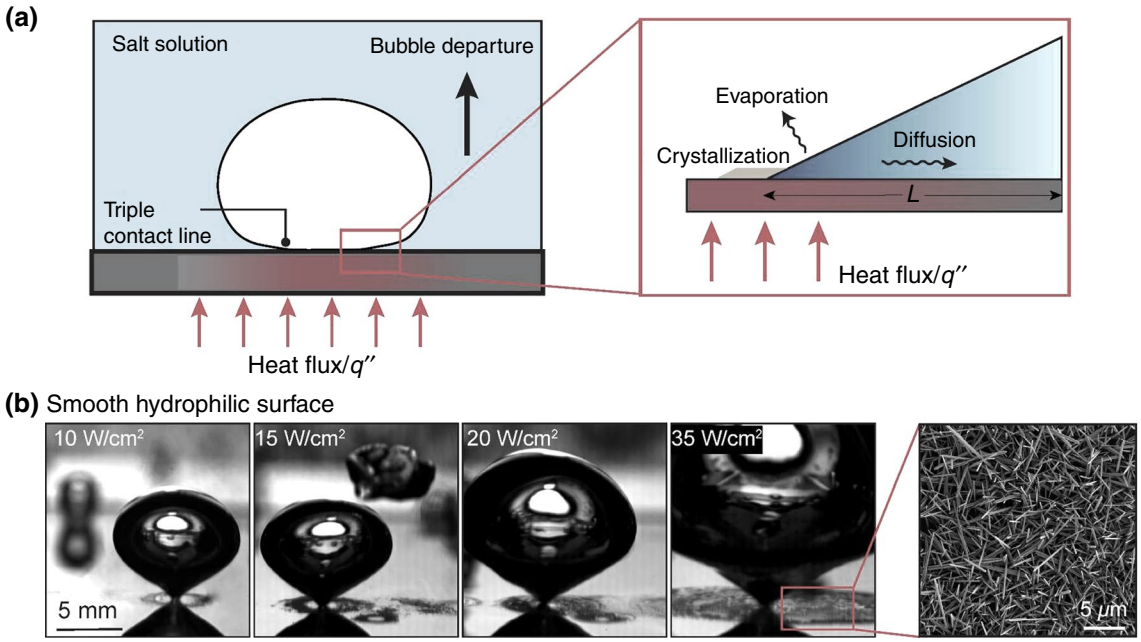

Fig. 11 **a** Schematic of bubble formation and transport mechanisms **b** bubble departure at variable heat flux for $CaSO_4$ solution [81]

Accuracy and uncertainty of equipment and experiments

Brace et al. [82] calculated the thermal effectiveness (ε) of overall fouling impact on the plate heat exchanger; they did analysis of error propagation using Eq. 12 throughout the experimental conditions, in which they assumed constant properties of the materials (i.e., fluid density and specific heat).

$$u(\varepsilon)^2 = \left(\frac{\partial \varepsilon}{\partial T_{\mathrm{h,\,in}}}\right)^2 u\left(T_{\mathrm{h,\,in}}\right)^2 + \left(\frac{\partial \varepsilon}{\partial T_{\mathrm{c,\,in}}}\right)^2 u\left(T_{\mathrm{c,\,in}}\right)^2 + \left(\frac{\partial \varepsilon}{\partial T_{\mathrm{c,\,out}}}\right)^2 u\left(T_{\mathrm{c,\,out}}\right)^2 + \left(\frac{\partial \varepsilon}{\partial \dot{\mathrm{m}}_{\mathrm{c}}}\right)^2 u\left(\dot{\mathrm{m}}_{\mathrm{c}}\right)^2 \tag{12}$$

They also provided a list of equipment with their uncertainty; for example, the fluid temperatures were measured by using K-type thermocouples with the uncertainty of ± 1.5 °C, the volume flow rate was measured by an electromagnetic flowmeter with the uncertainty of ± 1%, the electrical conductivity was monitored by an EC probe with the accuracy of 0.5%, the salt mass concentration was measured with the effectiveness of ± 0.56 mgL^{-1}, the surface temperature was measured by the infrared sensor with the accuracy of ± 2 °C and the thermal effectiveness (ε) was calculated by the specific equation which showed ± 4.42 to 5.23% uncertainty. Similarly, Shaikh et al., [83] provided the equipment preciseness in their study, such as they used heater setting temperature data with the accuracy of ± 0.05 °C, chiller temperature data with the accuracy of 0.1 °C, thermocouples with the precision of ± 1.5 °C, flowmeter with the measuring accuracy of ± 4% and data logger with the precision of 10 ms. Shengxian et al. [84] utilized the technical standard from literature to analyse the uncertainty of the acquired test data.

Fouling mitigation

Crystallization fouling provides serious negative impact on the heat transfer equipment, so the efficient cleaning or mitigation approaches are required to maintain appropriate capabilities of equipment during its lifespan. Figure 12 shows the several methods to deal with fouling in heat exchangers, from initial design to off-line cleaning. The selection of these approaches usually depends on the heat exchanger material, type, fouling mechanism, fouling severity, induced cost, desired results and operating conditions [85]. This study illustrates six fouling mitigation methods as mentioned in the following subsections.

Mitigation of fouling during the design of heat exchanger

If possible, fouling mitigation is preferred to adopt in the design process [86] while for efficacy of heat exchangers the fouling mitigation and cleaning approaches are also

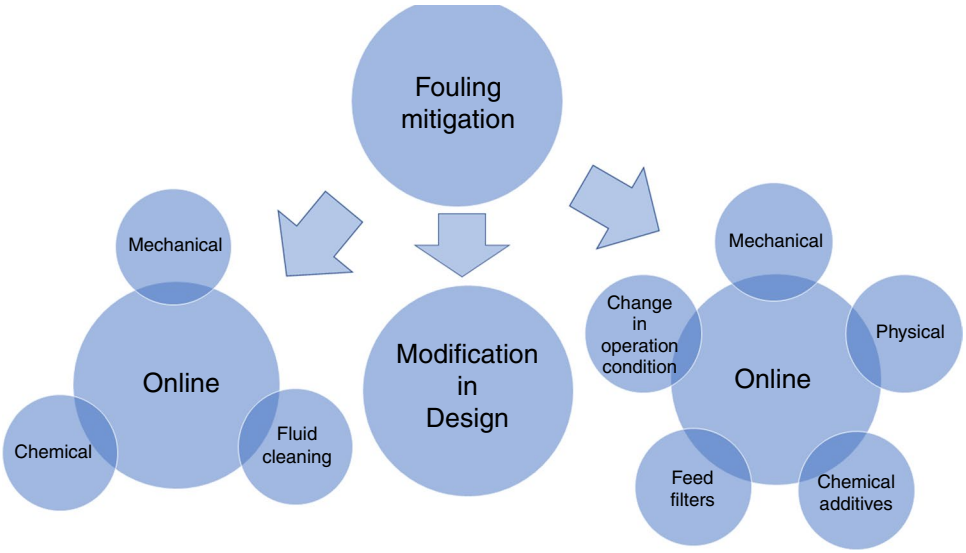

Fig. 12 Various methods to prevent fouling of heat exchangers

added. Field engineers and the engineering science data unit combinedly published design guidelines with these fouling processes for the assistance of manufacturers, as described by Pug et al. [27, 87]. The publications focus on bulk water fouling and illustrate the most frequently fouling mechanism, proposed range of operating values and influencing parameters for fouling. Procedures for selection of material, cleaning and mitigation of fouling are also given. Commonly recommended guidelines include construction of heat exchanger from the suitable materials and reduction of heat exchanger inside flow velocity. The freshwater heat exchangers from cast iron and carbon steel required significant maintenance during their lifespan.

So, to improve the performance of heat exchangers and the reduction of maintenance the alloy materials are recommended (i.e., stainless steels). For seawater system, copper alloys are commonly used. However, due to numerous benefits, use of titanium is increasing. Liquid–solid fluidized bed heat exchanger has been recently used for systems severely susceptible to fouling. where fluidized particles are incessantly striking the walls and removing the foulants. Maddahi et al. [88] studied fouling of $CaSO_4$ on liquid solid fluidized bed heat exchanger they also compared it with normally used forced convective heat transfer. Due to the particle and wall collision fouling was decreased remarkably and Heat transfer coefficient considerably increased. They also developed a model and validate with experimental data [89]. Such type of heat exchangers was also utilized in eutectic crystallization fouling [90, 91]. Change in heat exchanger type or design might cause huge expenses. So, off-line and online method can be used to the attain satisfactory operation such as different inhibitor agent, surface coating, off-line cleaning and miscellaneous method of inhabitation.

Mitigation of fouling by physical, chemical and mechanical treatment

Irrespective of the change in filtration and operating condition, for the mitigation purpose numerous physical, chemical and mechanical methods have been developed during the several years. Chemical inhibitors or agents are most frequently used due to commercial availability at the range of different conditions and suitability for all types of heat exchangers. Numerous comparisons exist between the chemical agents and the mitigators, based on the operating principle the chemical agents and the mitigators are classified into various groups (i.e., scale mitigators, pH controllers, surfactant or dispersants, ion exchangers, adsorption agents, antioxidants, oxidants, crystalline weaking agents and metal deactivators) [85]. Sousa and Bertran [92] assessed the fouling mitigator's performance with unceasing measurement of particle size distribution using laser diffraction and concomitantly pH recording. Polymeric mitigators, which work as both the nucleation and growth mitigators and show higher efficiency in comparison to the phosphonates which behave on growth principle. Shih et al. [93] evaluated five industrial anti-scalants using calcium and turbidity measurement. In induction time, considerable variations were observed due to the anti-scalant and its dosages. There are several drawbacks to use such types of chemicals, many of them may contain substance which can damage the environment or can react adversely with equipment material and produce cracks or corrosion [94]. These demerits can shift the approach to using of mechanical treatment such as wire brushes, sponge balls or different types of additions. Specific mitigation methods were used for the reduction of crystallization which occurs in the gas side of heat exchanger. Fouling species (i.e., sulphur, sodium or vanadium) from gasses can be removed before or after the gas combustion with several

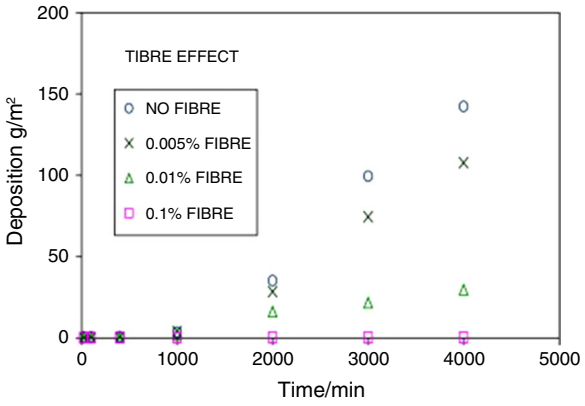

Fig. 13 Cumulative foulant deposition under the effect of different concentrations of fibre [28]

techniques. Soot blowers are used as a mechanical method for removal of gas fouling. Like liquid fouling, gas-side fouling influence is minimized through the control of important process parameters. The amount of excess air, surface temperature above the acidic dew point, elimination of flue gas and air fuel ratio are essentially controlled parameters [95].

Mitigation of foulants with additives

The inserts of non-crystallized particles into the bulk solution were also being investigated by different researchers and presented some inspiring results [96, 97]. Kazi et al. [28] added pulp of softwood fibre into the bulk solution which were found to retard the fouling deposition in association with the concentration of fibres added for all the tests as shown in Fig. 13. They also performed the experiments on addition of Arabic gum as additive which produced similar results on fouling inhibition as shown in Fig. 14 [98]. Teng et al. studied $CaCO_3$ fouling mitigation with the addition of EDTA [99] and DTPA [50] treated MWCNT-based nanofluid and obtained encouraging results as presented in Fig. 15, EDTA and DPTA treated MWCNT reduced the deposition of $CaCO_3$ on heat exchanger surface. Longer induction period was produced due to the increase in additive concentration, the calcium ion adsorption by additive was improved. Moreover, the EDTA-MWCNT additive enhanced the water thermal conductivity, which improved heat transfer. This improvement was achieved due to MWCNT, Brownain motion and water molecules formed surface nanolayers. Field emission scanning electron microscope (FESEM) images of the heat exchanger surfaces taken at 500X are shown in Fig. 16 depicts the crystal deposit morphology of surface with and without EDTA and MWCNT-EDTA additives. Figure 16 presents the FESEM image which shows that pointed, sharp and needlelike crystals were formed in case of the addition of additives, and in case of no addition of additives, larger crystals were formed. With the addition of additives, the deposit was smoother and duller, and the crystal size decreased. The metal surfaces were affected by MWCNT-EDTA oxidation and it incurred loss of mass. In comparison of EDTA additive, the higher concentrations of DPTA revealed zero corrosion and delivered better antifouling properties. It is known that the groundwater, seawater and river water contain metal ions such as Cu, iron and Pb. also cause harmful impact on the heat exchanger surfaces. Kazi et al. [21, 99] have suggested several additives to mitigate these metal ions fouling, such as EDTA-functionalized MWCNT and GNP, and DPTA-functionalized MWCNT and GNP. Xu et al. [58] effectively reduced $CaCO_3$ using sodium carboxymethyl cellulose (SCMC) additive in the bulk solution. The results showed the reduction in fouling rate and increase in the initiation period. Qian et al. [100] conducted a study on crystallization fouling of $CaCO_3$ in the appearance of soluble microbial products, produced from sulphate-reducing bacteria. At the concentration lower than

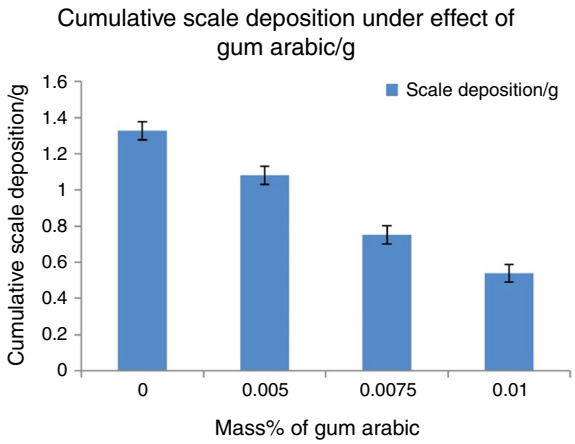

Fig. 14 Cumulative foulant deposition under the effect of different concentration of gum Arabic [98]

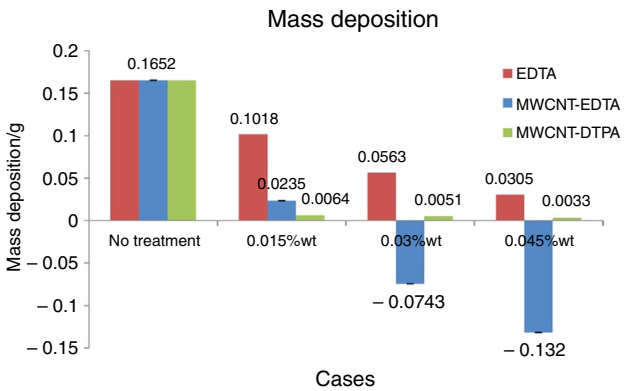

Fig. 15 Comparison of mass deposition under the effect of different concentration of EDTA, MWCNT-EDTA, MWCNT-DPTA [102]

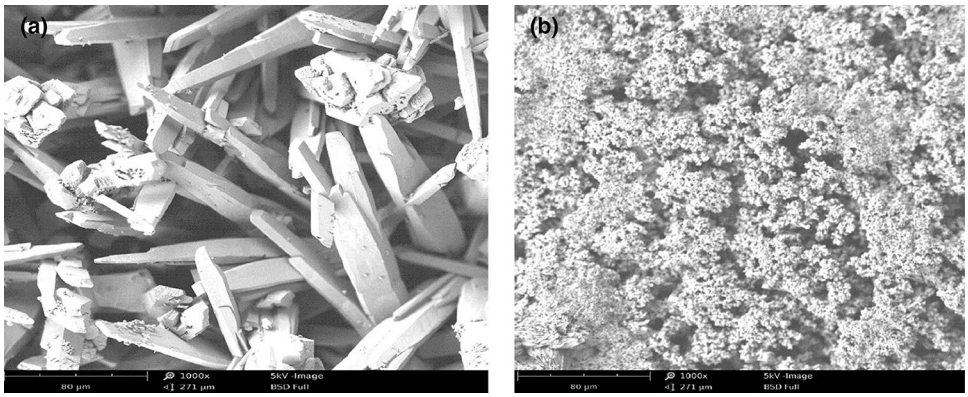

Fig. 16 FESEM Image of $CaCO_3$ deposit on SS 316L surface **a** without additive, **b** with MWCNT-EDTA additive [99]

the 8.79 mg L^{-1}, the soluble microbial products encouraged calcite calcification through chelation and when the content increased the growth of calcite formed in a peanut shape. In general, the results suggested that the microbial products are not favourable for $CaCO_3$ surface crystallization. Beneck et al. [101] analysed organic macromolecules antifouling impact of $CaSO_4$ on surface of reverse osmosis desalination experimental step up. Results revealed that the existence of macromolecules have transferred scaling mechanisms of gypsum from bulk solution to surface crystallization.

Mitigation of fouling using surface treatment

In the recent time, the focus of researchers has been transferred towards the surface treatments and development of advanced coating, for the mitigation of crystallize fouling. Al-Janabi and Malayari [62] assessed the impact of intermolecular interaction energies on $CaSO_4$ fouling with the modification of surface energy through four different types of surface coating. They established fundamental standards for surface energy on fouling and validate with their work. Same group has conducted a study on NI–P–BN coating which produced excellent results in reduction of adhesion forces among foulants deposits and surface. However, the coatings demonstrated considerable ageing, leading to poor abrasion resistance [103]. Yang et al.[104] investigated Ni–P–PTFE and Cu–DSA low energy surfaces and discovered that the fouling was reduced in comparison with uncoated copper surfaces. Later, they observed from the experiments that the weakening of adhesion delay in fouling can only be attained in induction period [105]. Cheng et al. [106] examined Ni–P monocrystalline and amorphous coatings, and discovered that both the coatings performed as reductant of tap water fouling. It was deemed that the properties of antifouling decreases with the increase in the monocrystalline phase share. In later study [107] the same research team investigated numerous PTFE content, such as Ni–Cu–P–PTFE under boiling flow conditions. Antifouling properties in coatings were found and investigators also observed that the fouling was promoted with the increase in surface free energy value. He et al. [108] studied hierarchical micro and nanoscale structured surfaces antifouling properties generated through electrical discharge machining (EDM). Results reveal that such treatment enhanced surface roughness, anti-corrosion properties and hydrophobicity. Results also depicted that at lower heat flux ranges, the induction period was considerably delayed in comparison with polished surfaces. Oon et al. [15] investigated stainless steel surface coating with titanium (chosen due to surface adhesion and high corrosion resistance) and found reduction in $CaCO_3$ deposition on the surface. Shaikh et al. [83] applied MWCNT mixture with gum Arabic on stainless steel surface (selected because of biodegradable nature of coating) and found decline in deposition of $CaCO_3$ and enhancement in overall heat transfer coefficient as shown in Figs. 17 and 18. Mayeret al. [109] assessed $CaCO_3$ adhesion forces on modified and unprocessed stainless steel surfaces, which can be utilized in detailed models of scaling.

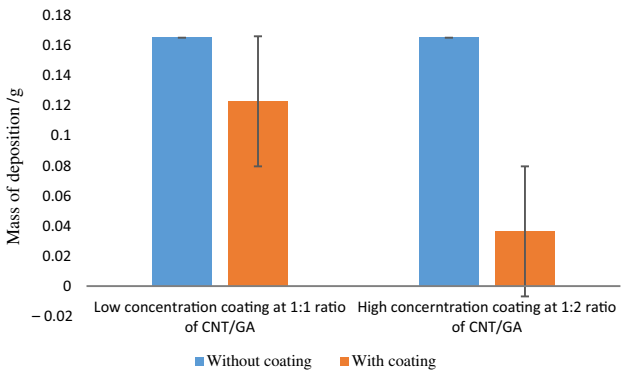

Fig. 17 Effect of coating on $CaCO_3$ mass deposition [83]

Mitigation of fouling through thermal shocks, electron antifouling, alternating electromagnetic field and combination of ultrasonic and alternating electromagnetic field

Vosough et al. [110] examined the mitigation of fouling through thermal shocks, when surface temperature suddenly increased or decreased. The results illustrate those thermal stresses due to shock, produced crack in fouling deposited layer and supports removal of foulant. Effectiveness of thermal shocks were observed at severe fouling condition. However, at lower bulk temperature, fouling concentration and heat flux, the thermal shocks were not helpful for removal of foulants. Electromagnetic water treatment experiments were also performed, a strongly diverging topic among the fouling investigators. Where numerous conflicting arguments are drawn. Wang and Liang [111] studied reduction of $CaCO_3$ deposition with alternating electromagnetic field. In U-shaped heat exchanger tube, the average diameter particles were significantly decreased with the application of such treatment. Fan et al. [112] examined the impact of water treatment with electronic antifouling (EAF) on crystallization fouling. In this water treatment technique, the pipe was wrapped with solenoid coil, through this treatment concentration of dissolved minerals were decreased by converting the minerals salts into insoluble crystals with the improvement in collusion process. In comparison to untreated water, fewer lager diameters crystals were produced in EAF treated water. Han et al. [57] studied impact of Mg^{2+} ion on precipitation of $CaCO_3$ with ultrasonic (US) and altering electromagnetic field (AEMF) treatment. They observed that the existence of Mg^{2+} ion can delay the calcium carbonate fouling and induction period. With the increase in the Mg^{2+}/Ca^{2+} ratio, the effect of ions increases. The team also suggested that considerable anti-scaling efficiency can be attained through the addition of suitable amount of Mg^{2+} ions with the combination of US + AEMF or AEMF + US treatment.

Fouling mitigation with off-line cleaning

Though the heat exchangers are designed with the consideration of fouling and the online mitigation is efficient, still the off-line cleaning is essential for some time. This off-line cleaning is normally attained through physical or chemical fluid cleaning methods as illustrated in Müller et al. [95]. As the mechanical cleaning methods requires the process shutdown, so, it is convenient to use it as occasionally as feasible. While planning the cleaning cycles a best possible balance among cleaning cost, process performance and reliability is needed. Several researchers reported about the optimization of cleaning cycle, emphasis was mainly given on one type of approach that fouling layer properties remain same throughout the lifespan of heat exchangers. In contrast to this strategy, gradual change in chemical and physical properties of fouling deposits needs to be reported in the suggested cleaning approaches. Epstein [113] considered the length among the consecutive cleaning cycles first-time, later some authors such as Pogiatzis et al. [114] adapted it and added the deposit ageing in it. The impact of ageing was included as enhancement in deposit layer which resist the chemicals; and in that consequence it is recommended for shifting the approach towards the mechanical cleaning. Like a single heat exchanger, networks cleaning approach can be optimized as revealed in the paper of Diaby et al. [115]. A strategy for network of 14 heat exchangers was invented under the variable ageing rates (slow and fast) using specific genetic algorithm. The approach produced considerable economic benefits mainly when deposit ageing affect at larger amount. The fouling cleaning depends on variation of input

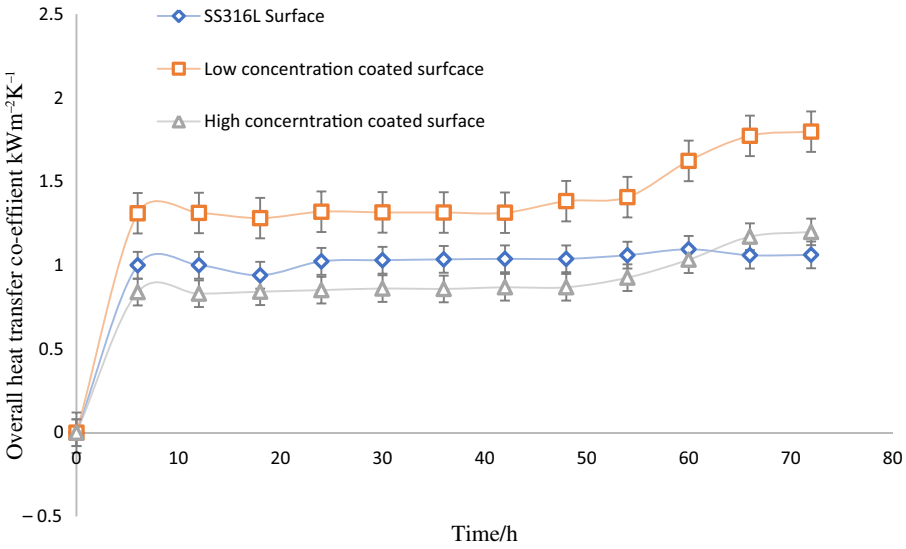

Fig. 18 Overall heat transfer coefficient for coated and non-coated surfaces [83]

quantities, i.e., the process parameters uncertainty. Various recommended cleaning approaches assume stable (steady-state) operations of heat exchanger and its network. Actually, the input quantities may fluctuate drastically and can significantly effect the optimization result. Pretoro et al. [116] established a normally used two-layer model (i.e., growing deposit is characterized through the sum of 2 layers with different properties and resistance to different cleaning techniques). For inlet hot temperature, Beta and Gaussian probability density functions were applied. The results illustrate a significant impact of probability functions on optimum cleaning cycle period and cost, emphasizing the significance of input parameters control in heat exchangers to be cleaned. Study conducted by Ismaili et al. [117] using various Gaussian distributions demonstrated similar outcomes. Significant inconsistency was found among the uncertainties or ignoring it in the estimates of optimum cleaning schedule of heat exchanger networks.

Fouling modelling

The present review demonstrates the transformation in fouling modelling from the early stages' observation phenomena to the more scientific method that started with the study of Kern and Seaton. Kern and Seaton developed a fouling model was one, from the earliest model [18]. This model assumed that the mass removal rate ($\dot{m}_r$) was proportional to the accumulated mass (m_f) while mass deposition rate ($\dot{m}_d$) was assumed constant with time t, and hence the mass deposition approach asymptotically with the increase in the time. Therefore,

Accumulation rate = Deposition rate − Removal rate.

Integration of Eq. 9 at initial condition $m_{f=}\,0$ and $t=0$ gives

$$m_f = m_F^*\left(1 - e^{-\beta t}\right) \tag{13}$$

where m_F^* is asymptotic accumulated mass, $\beta = 1/t_c$, t_c is time constant, which presents fouling element mean residence time on heat transfer surface. Using Eq. 10, Eq. 13 can be written as fouling resistance R_f at time t in the form of asymptotic fouling resistance R_f^*.

$$R_f = R_f^*\left(1 - e^{-\beta t}\right) \tag{14}$$

It is noticeable that the real solution needs to find R_f^* and t_c term as variable function affecting the fouling process.

In 1962, Hasson, through the study of $CaCO_3$ precipitation [118], considered crystallization fouling as a mass transfer process and suggested the growth rate ($\dot{m}_g$) model shown in Eq. 15:

$$\dot{m}_g = \frac{\left[\left\{Ca(HCO_3) - K_s'\right\}\right]}{\left(\frac{1}{K_m}\right) + \left(\frac{1}{K_r}\right)} \tag{15}$$

K_s' is deposit solubility product, K_m fluid–deposit mass transfer coefficient, K_r surface crystal forming reaction rate. K_m (can acquire from system geometry reliant empirical values) and product solubility (available in literature) allowed Hasson to use the measured growth rate for determination of reaction rate. He continued his research on the improvement of model and hypothesized that the deposition of $CaCO_3$ is predominantly controlled through Ca^{2+} and HCO^{3-} ion forward diffusion rate [119].

Crystallization fouling can usually be defined with the classical law of deposition rate where the rate of deposition ($\dot{m}_d$) is characterized as temperature reliant constant rate K_R^* and concentration driving force function; however, the influences of growth spots and nucleation were not considered.

$$\dot{m}_d = K_R^*\left(C_{fl} - C_{sat}\right)^n \tag{16}$$

Bansal et al. [120] investigated the above classical model with $CaSO_4$ crystallization fouling in plate heat exchanger and proposed a revised version:

$$\dot{m}_d = K_R^*\left(C_{fl} - C_{sat}\right)^n N\left(\frac{m_t}{m_{cg}}\right)^{n'} \tag{17}$$

where m_{cg} is the total mass deposit at the initial stage of crystal growth, m_t represents the total mass deposit after t time, n' is the exponent reliant on fouling situation and N represents the nucleation sites function (provided through particles in solution).

Kern and Seaton suggested the general crystallization fouling model that also tried the inclusion of surface energy in the model [121].

$$\dot{m}_d - \dot{m}_r = K_R^*\left(C_{fl} - C_{Sat}\right)^n C_1 \frac{\tau_{fl}}{\frac{1}{x_d}\left(W_a^* - \Delta E_{12}^{TOT}\right)} \tag{18}$$

where τ_{fl} symbolizes shear stress in fluid, x_d thickness of deposition, W_a^* deposit adhesion work on surface, ΔE_{12}^{TOT} total interaction energy among the surface and deposit. Bohnet [122] developed a model for second order reaction (i.e., precipitation of $CaSO_4$) by converting Eq. 11 in second order and then he simplified it with Eq. 16 for the development of second order model with the minimum variable requirements. The model predicts unlimited fouling layer growth, when both reaction rates and diffusion are running the process.

$$\dot{m}_{\mathrm{d}} = K_{\mathrm{m}}\left[\frac{1}{2}\left(\frac{K_{\mathrm{m}}}{K_{\mathrm{R}}}\right) + \left(C_{\mathrm{fl}} - C_{\mathrm{Sat}}\right) - \sqrt{\frac{1}{4}\left(\frac{K_{\mathrm{m}}}{K_{\mathrm{R}}}\right)^{2} + \left(\frac{K_{\mathrm{m}}}{K_{\mathrm{R}}}\right)\left(C_{\mathrm{fl}} - C_{\mathrm{Sat}}\right)}\right] \tag{19}$$

where rate of reaction K_{R} relies on the reaction order which could be defined with the Arrhenius equation, Sherwood number Sh and coefficient of diffusion D were used for the derivation of mass transfer coefficient K_{m}. C_{fl} and C_{sat} are the calcium sulphate concentration in the fluid and at the saturation level, respectively. For calcium carbonate species, scaling diffusion coefficient can be found in Segev et al. [123]. Meanwhile, other scientists particularly focused the induction period modelling [124].

Though the numerous models for crystallization fouling have been reported, almost all of them made one or more of the following generalization assumptions [51]:

- Assumed steady-state operation.
- Design and material of equipment are ignored.
- Roughness and induction delay period are not incorporated.
- Properties of fluid are assumed to be constant.
- Homogenous fouling layer is assumed.
- Deposits shape is not considered.
- Effect due to the change in flow cross section is not considered.
- Only single fouling mechanism is assumed.
- The effect of changing in surface area and surface roughness is ignored.

These models did not take effort to describe the basic fouling processes, but emphasis was given on quantification of various selected parameters in a particular test rig, where most of them are surface and bulk temperatures, flow velocity, time and concentration. Yang et al. [125] created a simplified empirical model for industrial crystallization fouling process characteristic. Jamialahmadi et al. [126] studied dehydration process fouling for the generation of phosphoric acid and suggested a systematic model for the improvement of cleaning process. Later, model was based on the impact of surface temperature, fluid velocity and concentration. Easvy and Malayeri [127] suggested a finned tube $CaSO_4$ scaling model during the nucleate pool boiling. Supersaturated microlayer under the bubbles as geometry function was calculated. The model results illustrated agreement with heat flux experimental data in between 100 and 300 kWm^{-2}. Babuška et al. [128] designed a $CaCO_3$ model that considers both temperature distribution and ageing in deposit. They involved ageing for removal of deposits and hence the model capable of presenting the results in sawtooth behaviour. Kapustenko et al. [129] create a model for prediction of particulate and precipitation fouling at various fouling temperature and flow velocity with and without increase of the heat transfer in plate heat exchanger. But model was not able to report the sizes and content of solid particulates or salt concentration. Kapustenko et al. also [129] developed a mathematical model for assessment of water fouling on plate heat exchangers. However, it needs the determination of numerous dimensionless constants. Souza and Costa [130] designed a cooling water system model, comprising of water pump, interconnected pipe section, cooling tower, and shell and tube heat exchangers. Reduction in the performance of entire system due to fouling were predicted. Bobič et al. [131] presents dynamic response model for counter flow plate heat exchanger under the condition of temperature fluctuations and external flow. Even though the model does not consider fouling, it offers attractive future control algorithm view for energy efficient heating and cooling application. This should be one which is capable of effectively predicting the fouling. Such algorithms can offer rapid response to an undesirable change in internal system (i.e., fouling above the set threshold limit) and respond suitably. Though there are plenty of sensible model and measurements exist, still several essential principles not explored, most of them yet to be verified in fundamental fouling study. These are perfectly developed general models and are able to define the crystallization fouling and its all-essential processes. But these are not suitable for the complex nature problem. Nevertheless, study on fundamentals of fouling is significant for the improvement of current model accuracy and enhancement of their usage to wider variety of affecting parameters.

In the last few years, researchers shifted their focus from single heat exchanger modelling to multiple or network heat exchangers modelling, which permits the significant industrial saving and supports the academia–industry collaboration [131]. Guelpa and Verda [132] designed a methodology for detection of fouling and examined it in six distribution network of heating system at Turin district. The model was capable of predicting the requirement of cleaning in any heat exchanger network, based on temperature on both side and mass flow on primary side, which are usually measured in district heating system. To adopt this methodology, there is no need to provide the data related to the type of heat exchanger, dimension, geometry and pressure drop. The team claimed that through the regular cleaning of heat exchangers the district network system can save up to 1.6% of primary energy consumption. Artificial neural networks are also demonstrating the encouraging results and considerably enhance the accuracy of some fouling models designed for industries. Davoudi and Vaferi [133] used ANNs for the systematic prediction of fouling level on heat exchanger, and here, the simplicity and small degree of error for large data experiment are key features of this model. Aguel et al.

[134] investigated the performance of heat exchangers in phosphoric acid concentrating plant and developed a model, which improved through backpropagation of ANN, where the model can be utilized for estimation of heat exchangers cleaning schedule. Sundar et al. [135] established a simplified and scalable mathematical model on the basis of deep learning for fouling resistance predication using normal measured parameters for heat exchangers in industries. The value of R^2, described how perfectly the model simulates the actual data, which was indicating more than 99% accuracy. Benyekhlef et al. [136] established an ANN model for estimation of MgO water and CuO water nanofluid effectiveness for reduction of fouling resistance in heat exchanger. With R^2 value, the results of model were described which represents more than 99% accuracy of model. Rohman et al. [137] utilized feed-forward neural network (FFNN) for estimation of fouling thickness in polyethylene tubular reactor. Result of model illustrate more than 98% accuracy for the prediction of fouling thickness. Though the ANNs were revealing the excellent earlier results, the field is still comparatively new, and publications related to fouling are rare. In the current years, CFD modelling software have also tremendously improved, which guided the utilization of CFD in fouling process modelling. The numerical method allows the computation of velocity gradient, local temperature and concentration in space and time, which have solid impact on fouling. Brahim et al. [138, 139] simulated $CaSO_4$ crystallization fouling on flat heater surface using CFD software. Though the ageing and initiating period was not incorporated, the CFD model still allowed appropriate fouling layer growth prediction and estimation of temperature distribution. Walker and Sheikholeslami [140] run the CFD model to describe the impact of flow velocity on bulk crystallization. Using this model, the radial concentration gradients was anticipated at laminar flow. Diffusive flux in radial direction was predicted owing to distribution of flow velocity in radial direction. As an alternative of the bulk solution, the crystallization was predominantly anticipated in viscous layers during the turbulent flow because of the enhanced in-residence time of particles in this lower flow velocity region. Xiao et al. [141] investigated induction period microscale fouling. This study focused on crystals growth with different density, shape, size, orientation, distribution and their impact on heat transfer and dynamic of flow. Compared to wider and shorter crystals, the slim and tall crystals were found for the enhancement of heat transfer in the induction period in a better way. Yang [142] examined the cured oil induction period fouling in tube heat exchanger. The influence of flow velocity and temperature was simulated with inclusion of formation, ageing and removal of fouling in model. Zhang et al. [143] run a CFD software to demonstrate the impact of main operating parameters on $CaSO_4$ fouling, i.e., foulant concentration, flow velocity, deposit porosity and inlet temperature. Haghshenasfard et al. [78] designed a subcooled flow boiling model, where they estimated the deposition of $CaSO_4$ on heated surface. The impact of flow velocity, surface roughness, surface temperature and fluid were anticipated. The model did not incorporate the enhancement in thermal resistance due to the rise in fouling layer. Ojaniemi et al. [144] developed a CFD model for the simulation of calcium phosphate fouling on plate heat exchanger. In this model precipitation of minerals were based on saturation ratio. Results of model agreed with experimental data. The accuracy of applied CFD model depends on input conditions, and if more fundamental processes are incorporated, then this CFD model become rapidly computationally demanding software. However, enhancing demand of computational software can be achieved through sudden advancements in processing field, demonstrating wide range of unexplored fouling simulation's future potential.

Cost imposed due to the fouling in terms of economic loss and environmental damage

Economic loss due to the fouling

Fouling imposes extra cost on industrial heat transfer equipment. In industries, cost related to the fouling have been determined by some studies. Cost of fouling can usually be divided into main five groups, i.e., (1) energy cost, (2) maintenance cost, (3) cost of production loss, (4) [145] cost of environmental management and (5) increased in capital expenditure [13]. Overall, cost of cleaning chemicals and equipment are imposing addition to maintenance cost of plants. The mechanical and chemical cleaning cost was assumed as 250 €/cleaning and 500 €/cleaning, respectively [146]. Cost of cleaning may vary from 700 to 1000 USD for a single heat exchanger [147, 148]. In China, fouling imposed annually 6065 USD/MW additional fuel cost due to energy production loss in power plant [149]. Fouling adds cost of 75,400 USD per km^2 for management of the environmental losses [148]. To compensate the fouling obstruction, heat transfer area of heat exchangers is kept surplus. Similarly, larger-size fans and pumps are selected to compensate the increase in the pressure loss from the reduction in flow area. One of the design approaches is to keep standby heat exchangers in design process to make sure operation are not interrupted when fouled heat exchangers are taken under fouling deposition cleaning maintenance [150]. Only in USA fouling in preheat train exchangers are responsible for 1.2 billion USD loss [30, 151]. Total cost due to fouling on heat exchangers for industrial globe was predicted as 5×10^{10} USD/year. Study conducted by Pretoro et al. [116] reported fouling cost in terms of 2018 gross national product (GNP)

Table 1 Fouling cost versus 2018 GNP [116]

S#	Country	Fouling cost/10^6 $/year	2018 GNP/10^6 $/year
1	USA	14,175	20,891,000
2	Germany	4875	4,356,353
3	New Zealand	64.5	197,827
4	Australia	463	1,318,153
5	France	2400	2,962,799
6	Japan	10,000	5,594,452

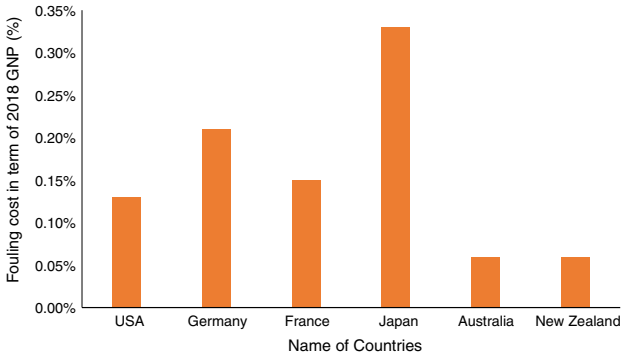

Fig. 19 Fouling impacts in terms of 2018 GNP % of different countries [116]

are shown in Table 1 and Fig. 19. Total yearly fouling cost for Japan is 0.33% of 2018 GNP and is highest among the other countries. For New Zealand and Australia, annually fouling cost is 0.06% of 2018 GNP of both countries and lowest among the other countries. In 2006, economic loss of China due to fouling in thermal power plants were 4.68 billion USD which was around 0.169% of GDP of China [149].

Environmental damage due to the fouling

Fewer scientists studied the effect of heat exchangers fouling on environment. Müller et al. [94] conduct a study on impacts of heat exchangers on environments. In this study, they said that fouling in exchangers' pipe creates many problems such as loss in heat transfer, under-deposit corrosion, flow maldistribution and pressure drop. All these have not only negative impacts on economy of plants but also have direct and indirect impact on environment. Disposal of foulant and additive used for reduction of fouling can create water and land pollution. ESDU reported that crude oil refineries in USA are responsible for 7 million tonnes of CO_2 emissions due to fouling [151]. Elwerfalli [148] found that the schedule shutdown for removal of fouling damaged the environment within 5 kms radius. Casanueva-Robles and Bott [152] found that with the increase in the fouling thickness in condenser of power plant, emissions of carbon dioxide increased. They found that1000 μm fouling thickness, raised the emission rate by almost 2900 tonnes of CO_2/h. Due to increase in fouling, heat exchangers required more electrical power and in most of industries electrical power is produced using fossil fuels that emits different hazardous gasses (i.e., CO_2, CO, SO_x and NO_x.) which are hazardous for both environment and human health.

Future direction

Future investigation of two or more composite fouling mitigation and modelling approach will enhance the research background related to various factors that affect the fouling mitigation process and sophisticated new eco-friendly mitigation process for future applications. Therefore, developing of efficient, economical, eco-friendly carbon-based additives from biodegradable waste and their composite for the mitigation of deposits on heat exchanger surface is always crucial. Additionally, new methods for mechanical and fluid cleaning, coating of heat transfer surface with new eco-friendly, corrosion resistive and composite nanomaterials such as GNP, CNT and hybrid of these through different techniques (i.e., powder physical vapour deposition, electrophoresis, and dip and spray coating) and alteration of design and operating conditions will help scientists in future studies. Furthermore, modelling of composite fluid using latest technology such as CFD, ANN, fuzzy logic, genteic algorthim (GA) and particle swarm optimization (PSO) will reduce the cost of experiments and challenges faced by previous fouling modelling attempts. Moreover, toxicity and risk assessment of nanoadditive, assessment of reduction in CO_2, NO_x and SO_x emissions and economic benefits due to mitigation of foulants should be carried out through life cycle assessment (LCA) for provision of more environmental and economic benefits.

Conclusions

In recent years, people are gradually moving towards the carbon neutralization. In this regard, fouling is not adequately considered, though the fouling in condenser of powerplants alone increases tonnes of CO_2 emissions. If this cause is not adequate for consideration, fouling also imposed cost as 0.33% of 2018 gross national products (GNP) of highly industrialized countries. These two reasons together with numerous others, warning to pay more attention towards fouling and its mitigation measures should be noted. Most design engineers ignored the fundamental information

about crystallize foulants and pay greater attention to fouling mitigation approaches. But studies on fundamentals of fouling can provide greater benefit in designing of future heat exchangers. The models are mostly developed from experimental investigation or based on partially empirical assumptions. Computational fluid dynamics (CFD) simulator and neural network will be vital when these fundamental processes are adequately explained to forecast future process in better way. Various mitigation methods were established through different experiments, which demands further awareness on operating principles; therefore, fouling can only be reduced but never fully prevented. Hence, the requirement of better and new approaches is always necessary for the present and will be required in the future.

Acknowledgements This study is supported financially under the Fundamental Research Grant Scheme awarded by the Ministry of Higher Education Malaysia with Grant Number: FRGS/1/2019/TK03/UM/02/12 (FP143-2019A). The authors also gratefully acknowledge the support from Grants, RMF0400-13-2021, ST049-2022, RK001-2022, Centre of Advanced Manufacturing and Material Processing (AMMP), Centre for Energy Sciences(CES), Centre of Advanced Materials (CAM), Department of Mechanical Engineering, Universiti Malaya, and BUITEMS, Pakistan to conduct this research work.

References

1. Helalizadeh A, Müller-Steinhagen H, Jamialahmadi M. Mixed salt crystallisation fouling. Chem Eng Process Process Intensif. 2000;39:29–43.
2. Arasteh H, Mashayekhi R, Ghaneifar M, Toghraie D, Afrand M. Numerical simulation of heat transfer enhancement in a plate-fin heat exchanger using a new type of vortex generators. J Therm Anal Calorim. 2020;141:1669–85. https://doi.org/10.1007/s10973-019-08870-w.
3. Kazi SN, Duffy GG, Chen XD. Mineral scale formation and mitigation on metals and a polymeric heat exchanger surface. Appl Therm Eng. 2010;30:2236–42. https://doi.org/10.1016/j.applthermaleng.2010.06.005.
4. Zhao X, Chen XD. A Critical Review of basic crystallography to salt crystallization fouling in heat exchangers. Heat Transf Eng. 2013;34:719–32.
5. Berce J, Zupančič M, Može M, Golobič I. A review of crystallization fouling in heat exchangers. Processes. 2021;9:66.
6. Bott TR. Fouling Note Book [Internet]. Rugby United Kingdom; 1990. https://www.osti.gov/etdeweb/biblio/5299249.
7. Albert F, Augustin W, Scholl S. Roughness and constriction effects on heat transfer in crystallization fouling. Chem Eng Sci. 2011;66:499–509. https://doi.org/10.1016/j.ces.2010.11.021.
8. Förster M, Augustin W, Bohnet M. Influence of the adhesion force crystal/heat exchanger surface on fouling mitigation. Chem Eng Process Process Intensif. 1999;38:449–61.
9. Helalizadeh A, Müller-Steinhagen H, Jamialahmadi M. Mathematical modelling of mixed salt precipitation during convective heat transfer and sub-cooled flow boiling. Chem Eng Sci. 2005;60:5078–88.
10. Bansal B, Chen XD, Muller-Steinhagen H. Deposition and removal mechanisms during calcium sulfate fouling in heat exchangers. Int J Transp Phenom. 2005;7:1–22.
11. Heberle A, Schaber K. Modeling of fouling on packings in absorption columns. AIChE J. 2002;48:2722–31.
12. Muller-Steinhagen H. The ultimate challenge for heat exchanger design. In: 6th International symposium transport phenomena thermal engineering. Seoul Korea; 1993. p. 811–23.
13. Kazi SN. Fouling and fouling mitigation of calcium compounds on heat exchangers by novel colloids and surface modifications. Rev Chem Eng. 2020;36:653–85.
14. Vosough A, Assari MR, Peyghambarzadeh SM. Experimental measurement of heat transfer coefficient and mass of deposited $CaSO_4$ in subcooled flow boiling condition. J Comput Appl Mech. 2019;50:308–14.
15. Oon CS, Kazi SN, Hakimin MA, Abdelrazek AH, Mallah AR, Low FW, et al. Heat transfer and fouling deposition investigation on the titanium coated heat exchanger surface. Poweder Technol. 2020;373:671–80. https://doi.org/10.1016/j.powtec.2020.07.010.
16. Song KS, Lim J, Yun S, Kim D, Kim Y. Composite fouling characteristics of $CaCO_3$ and $CaSO_4$ in plate heat exchangers at various operating and geometric conditions. Int J Heat Mass Transf. 2019;136:555–62. https://doi.org/10.1016/j.ijheatmasstransfer.2019.03.032.
17. Singh A. Heat Exchanger Fouling By Precipitation Of Calcium Phosphates By Atmajeet Singh B. Tech., Indian Institute of Technology, New Delhi, India; A Thesis in Partial Fulfilment of the Requirements for the Degree of Master of Applied Science in the Faculty Office; 1992.
18. Kern D. A theoretical analysis of thermal surface fouling. Br Chem Eng. 1959;4:258–62.
19. Kazi MSN. Heat transfer to fibre suspensions: studies in fibre characterisation and fouling mitigation. University of Aukland; 2001.
20. Epstein N. Thinking about heat transfer fouling: a 5 × 5 matrix. Heat Transf Eng. 1983;4:43–56.
21. Kazi SN. Water-formed deposits fundamentals and mitigation strategies. Koch A, editor. Susan Dennis; 2022.
22. Taborek J, Hewitt GF, Afgan N. Heat exhangers: theory and practice. Washington, DC: Hemisphere Publishing Corp; 1983.
23. Melo LF, Bott TR, Berando CA. Fouling science and technology. North Atl Treaty Organ Sci Aff Div [Internet]. Alvor, Algarve, Portugal; 1988. https://www.worldcat.org/title/fouling-science-and-technology/oclc/17954359
24. Shah RK. Research needs in low Reynolds number flow heat exchangers. Heat Transf Eng. 1981;3:49–61.
25. Coletti F, Crittenden BD, Macchietto S. Basic science of the fouling process. Crude Oil Fouling Depos Charact Meas Model. 2015. https://doi.org/10.1016/B978-0-12-801256-7.00002-6.
26. Geddert T, Bialuch I, Augustin W, Scholl S. Extending the induction period of crystallization fouling through surface coating. Heat Transf Eng. 2009;30:868–75.
27. Pugh SJ, Hewitt GF, Müller-Steinhagen H. Fouling during the use of seawater as coolant—the development of a user guide. Heat Transf Eng. 2005;26:35–43.
28. Kazi SN. Fouling and fouling mitigation on heat exchanger surfaces. Heat Exch Basics Des Appl. 2012;66:6.
29. Besevic P, Clarke SM, Kawaley G, Wilson DI. Effect of silica on deposition and ageing of calcium carbonate fouling layers. Heat Exch Fouling Clean. 2017;66:58–66.
30. Sileri D, Sahu K, Ding H, Matar OK. Mathematical modelling of asphatenes deposition and removal in crude distillation units. In: International conference heat exchange fouling Clean VIII. 2009. p. 245–51.
31. Lv Y, Lu K, Ren Y. Composite crystallization fouling characteristics of normal solubility salt in double-pipe heat exchanger. Int J Heat Mass Transf. 2020;66:156.

32. Choi Y, Naidu G, Jeong S, Lee S, Vigneswaran S. Effect of chemical and physical factors on the crystallization of calcium sulfate in seawater reverse osmosis brine. Desalination. 2018;426:78–87. https://doi.org/10.1016/j.desal.2017.10.037.
33. Chong TH, Sheikholeslami R. Thermodynamics and kinetics for mixed calcium carbonate and calcium sulfate precipitation. Chem Eng Sci. 2001;56:5391–400.
34. Al-Gailani A, Sanni O, Charpentier TVJ, Crisp R, Bruins JH, Neville A. Examining the effect of ionic constituents on crystallization fouling on heat transfer surfaces. Int J Heat Mass Transf. 2020;160:120180. https://doi.org/10.1016/j.ijheatmasstransfer.2020.120180.
35. Krömer K, Will S, Loisel K, Nied S, Detering J. Scale formation and mitigation of mixed salts in horizontal tube falling film evaporators for seawater desalination scale formation and mitigation of mixed salts in horizontal tube falling film evaporators for seawater desalination. Heat Transf Eng. 2015;66:37–41.
36. Lugo-Granados H, Tamakloe EK, Picón-Núñez M. Controlling scaling in heat exchangers through the use of fouling design curves. Process Integr Optim Sustain. 2020;4:111–20.
37. Kazi SN, Duffy GG, Chen XD. Fouling and fouling mitigation on different heat exchanging. In: Proceedings of the international conference heat exchange fouling cleaning VIII—2009. 2009. p. 367–77.
38. Hou TK. Fouling and its mitigation on heat exchanger surfaces by additives and catalytic materials Teng Kah Hou A thesis submitted in partial fulfillment of the requirements of Liverpool John Moores University for the degree of Doctor of Philosophy This research; 2018.
39. Höfling V, Augustin W, Bohnet M. Heat exchanger fouling and cleaning: fundamentals and applications crystallization fouling of the aqueous. 2003.
40. Augustin W, Bohnet M. Effect of pH-value on fouling behaviour of heat exchangers. 2018.
41. Schnöing L, Augustin W, Scholl S. Fouling mitigation in food processes by modification of heat transfer surfaces: a review. Food Bioprod Process. 2020;121:1–19. https://doi.org/10.1016/j.fbp.2020.01.013.
42. Schoenitz M, Grundemann L, Augustin W, Scholl S. Fouling in microstructured devices: a review. Chem Commun. 2015;51:8213–28. https://doi.org/10.1039/C4CC07849G.
43. Wray JL, Daniels F. Precipitation of calcite and aragonite. J Am Chem Soc. 1957;79:2031–4.
44. Wang G, Zhu L, Liu H, Li W. Zinc-graphite composite coating for anti-fouling application. Mater Lett. 2011;65:3095–7. https://doi.org/10.1016/j.matlet.2011.06.096.
45. Sheikholeslami R, Ng M. Calcium sulfate precipitation in the presence of nondominant calcium carbonate: thermodynamics and kinetics. Ind Eng Chem Res. 2001;40:3570–8.
46. Dong L, Crittenden BD, Yang M. Fouling characteristics of water–$CaSO_4$ solution under surface crystallization and bulk precipitation. Int J Heat Mass Transf. 2021;66:180.
47. Ataki A, Kiepfer H, Bart HJ. Investigations on crystallization fouling on PEEK films used as heat transfer surfaces: experimental results. Heat Mass Transf und Stoffuebertragung Heat Mass Transf. 2020;56:1443–52.
48. Hatch G. Evaluation of scaling tendencies. Mater Prot Perform. 1973;12:49–50.
49. Hasson D, Zahavi J. Mechanislm of calcium sulfate scale deposition o n heat-transfer surfaces. Ind Eng Chem Fundam. 1970;9:1–10.
50. Teng KH, Kazi SN, Amiri A, Habali AF, Bakar MA, Chew BT, et al. Calcium carbonate fouling on double-pipe heat exchanger with different heat exchanging surfaces. Powder Technol. 2017;315:216–26. https://doi.org/10.1016/j.powtec.2017.03.057.
51. Kazi SN, Duffy GG, Chen XD. Fouling and fouling mitigation on heated metal surfaces. Desalination. 2012;288:126–34. https://doi.org/10.1016/j.desal.2011.12.022.
52. Al-Gailani A, Sanni O, Charpentier TVJ, Crisp R, Bruins JH, Neville A. Inorganic fouling of heat transfer surface from potable water during convective heat transfer. Appl Therm Eng. 2021;184:116271. https://doi.org/10.1016/j.applthermaleng.2020.116271.
53. Ren L, Cheng Y, Wang Q, Tian X, Yang J, Zhang D. Relationship between corrosion product and fouling growth on mild steel, copper and brass surface. Colloids Surf A Physicochem Eng Asp. 2020;124–502. https://doi.org/10.1016/j.colsurfa.2020.124502
54. Ren L, Cheng Y, Wang Q, Yang J. Simulation of the relationship between calcium carbonate fouling and corrosion of iron surface. Colloids Surfaces A Physicochem Eng Asp. 2019;66:1238825. https://doi.org/10.1016/j.colsurfa.2019.123882.
55. Wang J, Wang L, Miao R, Lv Y, Wang X, Meng X, et al. Enhanced gypsum scaling by organic fouling layer on nanofiltration membrane: characteristics and mechanisms. Water Res. 2016;91:203–13. https://doi.org/10.1016/j.watres.2016.01.019.
56. Cooper A, Suitor JW, Usher JD. Cooling water fouling in plate heat exchangers. Heat Transf Eng. 1980;1:50–5.
57. Han Z, Xu Z, Wang J. CaSO4 fouling characteristics on the rectangular channel with half-cylinder vortex generators. Appl Therm Eng. 2018;128:1456–63. https://doi.org/10.1016/j.applthermaleng.2017.09.051.
58. Xu Z, Zhao Y, Wang J, Chang H. Inhibition of calcium carbonate fouling on heat transfer surface using sodium carboxymethyl cellulose. Appl Therm Eng. 2019;148:1074–80. https://doi.org/10.1016/j.applthermaleng.2018.11.088.
59. Hasan BO, Nathan GJ, Ashman PJ, Craig RA, Kelso RM. The use of turbulence generators to mitigate crystallization fouling under cross flow conditions. Desalination. 2012;288:108–17. https://doi.org/10.1016/j.desal.2011.12.019.
60. Samadifar M, Toghraie D. Numerical simulation of heat transfer enhancement in a plate-fin heat exchanger using a new type of vortex generators. Appl Therm Eng. 2018;133:671–81. https://doi.org/10.1016/j.applthermaleng.2018.01.062.
61. Hasan BO, Jwair EA, Craig RA. The effect of heat transfer enhancement on the crystallization fouling in a double pipe heat exchanger. Exp Therm Fluid Sci. 2017;86:272–80. https://doi.org/10.1016/j.expthermflusci.2017.04.015.
62. Al-Janabi A, Malayeri MR. A criterion for the characterization of modified surfaces during crystallization fouling based on electron donor component of surface energy. Chem Eng Res Des. 2015;100:212–27. https://doi.org/10.1016/j.cherd.2015.05.033.
63. Großerichter D, Stichlmair J. Crystallization fouling in packed columns. Chem Eng Res Des. 2003;81:68–73.
64. Zhao L, Tang W, Wang L, Li W, Minkowycz WJ. Heat transfer and fouling characteristics during falling film evaporation in a vertical sintered tube. Int Commun Heat Mass Transf. 2019;109:104388. https://doi.org/10.1016/j.icheatmasstransfer.2019.104388.
65. Zettler HU, Weiß M, Zhao Q, Müller-Steinhagen H. Influence of surface properties and characteristics on fouling in plate heat exchangers. Heat Transf Eng. 2005;26:3–17.
66. Feurstein G, Rampf HM. Der Einfluss rechteckiger Rauhigkeiten auf den Waermeuebergang und den Druckabfall in turbulenter Ringspaltstroemung. 1969;2:19–30.
67. Taylor RP, Hosni MH, Garner JW, Coleman HW. Thermal boundary condition effects on heat transfer in turbulent rough-wall boundary layers. Wärme - und Stoffübertragung. 1992;27:131–40.

68. Augustin M, Bohnet W. Effect of surface structure and ph-value on fouling behaviour of heat exchangers. Transp Phenom Therm Eng. 1993;2:884–9.
69. Sheriff N, Gumley P. Heat-transfer and friction properties of surfaces with discrete roughnesses. Int J Heat Mass Transf. 1966;9:1297–320.
70. Lei C, Peng Z, Day T, Yan X, Bai X, Yuan C. Experimental observation of surface morphology effect on crystallization fouling in plate heat exchangers. Int Commun Heat Mass Transf. 2011;38:25–30. https://doi.org/10.1016/j.icheatmasstransfer.2010.10.006.
71. Yoon J, Lund DB. Magnetic treatment of milk and surface treatment of plate heat exchangers: effects on milk fouling. J Food Sci. 1994;59:964–9.
72. McGuire J, Swartzel KR. On the use of water in the measurement of solid surface tension. Surf Interface Anal. 1987;10:430–3.
73. Herz A, Malayeri MR, Müller-steinhagen H. Fouling of roughened stainless steel surfaces during convective heat transfer to aqueous solutions. Energy Convers Manag. 2008;49:3381–6.
74. Al-otaibi DA, Hashmi MSJ, Yilbas BS. Fouling resistance of brackish water: comparision of fouling characteristics of coated carbon steel and titanium tubes. Exp Therm Fluid Sci. 2014;55:158–65. https://doi.org/10.1016/j.expthermflusci.2014.03.010.
75. Abd-Elhady MS, Malayeri MR. Transition of convective heat transfer to subcooled flow boiling due to crystallization fouling. Appl Therm Eng. 2016;92:122–9. https://doi.org/10.1016/j.applthermaleng.2015.09.093.
76. Rashidi S, Hormozi F, Mohsen M. Fundamental and subphenomena of boiling heat transfer. J Therm Anal Calorim. 2020;6:66. https://doi.org/10.1007/s10973-020-09468-3.
77. Malayeri MR, Müller-steinhagen H, Bartlett TH. Fouling of tube bundles under pool boiling conditions. Chem Eng Sci. 2005;60:1503–13.
78. Haghshenasfard M, Yeoh GH, Dahari M, Hooman K. On numerical study of calcium sulphate fouling under sub-cooled flow boiling conditions. Appl Therm Eng. 2015. https://doi.org/10.1016/j.applthermaleng.2015.01.079.
79. Peyghambarzadeh SM, Vatani A, Jamialahmadi M. Application of asymptotic model for the prediction of fouling rate of calcium sulfate under subcooled fl ow boiling. Appl Therm Eng. 2012;39:105–13. https://doi.org/10.1016/j.applthermaleng.2011.12.042.
80. Chen JC. Transfer to saturated fluids in convective flow. 1966.
81. Dash S, Rapoport L, Varanasi KK. Crystallization-induced fouling during boiling: formation mechanisms to mitigation approaches. Langmuir. 2018;34:782–8.
82. Berce J, Mo M, Golobi I. Infrared thermography observations of crystallization fouling in a plate heat exchanger. 2023. p. 224.
83. Shaikh K, Kazi SN, Mohd Zubir MN, Wong K, Binti Mohd Yusoff SA, Ahmed Khan W, et al. Mitigation of $CaCO_3$ fouling on heat exchanger surface using green functionalized carbon nanotubes (GFCNT) coating. Therm Sci Eng Prog. 2023;42:101–878.
84. Cao S, Zou M, Zhao B, Gao H, Wang G. Investigation of corrosion and fouling resistance of Ni–P-nanoparticles composite coating using online monitoring technology. Elsevier Masson SAS; 2023. p. 184.
85. Müller-Steinhagen H, Malayeri MR, Watkinson AP. Heat exchanger fouling: mitigation and cleaning strategies. Heat Transf Eng. 2011;32:189–96.
86. Miansari M, Valipour MA, Arasteh H, Toghraie D. Energy and exergy analysis and optimization of helically grooved shell and tube heat exchangers by using Taguchi experimental design. J Therm Anal Calorim. 2020;139:3151–64. https://doi.org/10.1007/s10973-019-08653-3.
87. Pugh SJ, Hewitt GF, Müller-Steinhagen H. Fouling during the use of fresh water as coolant the development of a user guide. Heat Transf Eng. 2009;30:851–8.
88. Maddahi MH, Hatamipour MS, Jamialahmadi M. Experimental study of calcium sulfate fouling in a heat exchanger during liquid–solid fluidized bed with cylindrical particles. Int J Therm Sci. 2018;125:11–22. https://doi.org/10.1016/j.ijthermalsci.2017.11.007.
89. Maddahi MH, Hatamipour MS, Jamialahmadi M. A model for the prediction of thermal resistance of calcium sulfate crystallization fouling in a liquid–solid fluidized bed heat exchanger with cylindrical particles. Int J Therm Sci. 2019;145:106017. https://doi.org/10.1016/j.ijthermalsci.2019.106017.
90. Pronk P, Infante Ferreira CA, Witkamp GJ. Mitigation of ice crystallization fouling in stationary and circulating liquid–solid fluidized bed heat exchangers. Int J Heat Mass Transf. 2010;53:403–11. https://doi.org/10.1016/j.ijheatmasstransfer.2009.09.016.
91. Pronk P, Infante Ferreira CA, Witkamp GJ. Prevention of crystallization fouling during eutectic freeze crystallization in fluidized bed heat exchangers. Chem Eng Process Process Intensif. 2008;47:2140–9.
92. Sousa MFB, Bertran CA. New methodology based on static light scattering measurements for evaluation of inhibitors for in bulk $CaCO_3$ crystallization. J Colloid Interface Sci. 2014;420:57–64. https://doi.org/10.1016/j.jcis.2014.01.001.
93. Shih W-Y, Albrecht K, Glater J, Cohen Y. A dual-probe approach for evaluation of gypsum crystallization in response to antiscalant treatment. Desalination. 2004;169:213–21.
94. Müller-Steinhagen H, Malayeri MR, Watkinson AP. Heat exchanger fouling: environmental impacts. Heat Transf Eng. 2009;30:773–6.
95. Müller-Steinhagen H. Heat transfer fouling: 50 years after the Kern and Seaton model. Heat Transf Eng. 2011;32:1–13.
96. Moradi A, Toghraie D, Isfahani AHM, Hosseinian A. An experimental study on MWCNT–water nanofluids flow and heat transfer in double-pipe heat exchanger using porous media. J Therm Anal Calorim. 2019;137:1797–807. https://doi.org/10.1007/s10973-019-08076-0.
97. Shahsavar A, Godini A, Sardari PT, Toghraie D, Salehipour H. Impact of variable fluid properties on forced convection of Fe_3O_4/CNT/water hybrid nanofluid in a double-pipe mini-channel heat exchanger. J Therm Anal Calorim. 2019;137:1031–43. https://doi.org/10.1007/s10973-018-07997-6.
98. Kazi SN, Teng KH, Zakaria MS, Sadeghinezhad E, Bakar MA. Study of mineral fouling mitigation on heat exchanger surface. Desalination. 2015;367:248–54. https://doi.org/10.1016/j.desal.2015.04.011.
99. Teng KH, Amiri A, Kazi SN, Bakar MA, Chew BT. Fouling mitigation on heat exchanger surfaces by EDTA-treated MWCNT-based water nanofluids. J Taiwan Inst Chem Eng. 2016;60:445–52. https://doi.org/10.1016/j.jtice.2015.11.006.
100. Qian J, Wang J, Yue Z, Wu W. Surface crystallization behavior of calcium carbonate in the presence of SMPs secreted by SRB. J Cryst Growth. 2019;525:125208. https://doi.org/10.1016/j.jcrysgro.2019.125208.
101. Benecke J, Rozova J, Ernst M. Anti-scale effects of select organic macromolecules on gypsum bulk and surface crystallization during reverse osmosis desalination. Sep Purif Technol. 2018;198:68–78. https://doi.org/10.1016/j.seppur.2016.11.068.
102. Teng KH, Amiri A, Kazi SN, Bakar MA, Chew BT, Al-Shamma'a A, et al. Retardation of heat exchanger surfaces mineral fouling by water-based diethylenetriamine pentaacetate-treated CNT

nanofluids. Appl Therm Eng. 2017;110:495–503. https://doi.org/10.1016/j.applthermaleng.2016.08.181.
103. Al-Janabi A, Malayeri MR, Müller-Steinhagen H. Experimental fouling investigation with electroless Ni–P coatings. Int J Therm Sci. 2010;49:1063–71.
104. Yang Q, Ding J, Shen Z. Investigation on fouling behaviors of low-energy surface and fouling fractal characteristics. Chem Eng Sci. 2000;55:797–805.
105. Yang Q, Liu Y, Gu A, Ding J, Shen Z. Investigation of induction period and morphology of $CaCO_3$ fouling on heated surface. Chem Eng Sci. 2002;57:921–31.
106. Cheng YH, Zou Y, Cheng L, Liu W. Effect of the microstructure on the anti-fouling property of the electroless Ni–P coating. Mater Lett. 2008;62:4283–5.
107. Cheng YH, Chen HY, Zhu ZC, Jen TC, Peng YX. Experimental study on the anti-fouling effects of Ni–Cu–P–PTFE deposit surface of heat exchangers. Appl Therm Eng. 2014;68:20–5. https://doi.org/10.1016/j.applthermaleng.2014.04.003.
108. He ZR, Liu CS, Gao HY, Jie XH, Lian WQ. Experimental study on the anti-fouling effects of EDM machined hierarchical micro/nano structure for heat transfer surface. Appl Therm Eng. 2019;162:66.
109. Mayer M, Bucko J, Benzinger W, Dittmeyer R, Augustin W, Scholl S. The impact of crystallization fouling on a microscale heat exchanger. Exp Therm Fluid Sci. 2012;40:126–31. https://doi.org/10.1016/j.expthermflusci.2012.02.007.
110. Vosough A, Peyghambarzadeh SM, Assari MR. Influence of thermal shock on the mitigation of calcium sulfate crystallization fouling under subcooled flow boiling condition. Appl Therm Eng. 2020;164:114434. https://doi.org/10.1016/j.applthermaleng.2019.114434.
111. Wang J, Liang Y. Anti-fouling effect of axial alternating electromagnetic field on calcium carbonate fouling in U-shaped circulating cooling water heat exchange tube. Int J Heat Mass Transf. 2017;115:774–81. https://doi.org/10.1016/j.ijheatmasstransfer.2017.07.097.
112. Fan C, Cho YI. Microscopic observation of calcium carbonate particles: validation of an electronic anti-fouling technology. Int Commun Heat Mass Transf. 1997;24:747–56.
113. Epstein RSTM and N. Optimum cycles for falling rate processes. Depertment chmeical Eng Univ Birtish Colomb. 1981. p. 631–3.
114. Pogiatzis T, Ishiyama EM, Paterson WR, Vassiliadis VS, Wilson DI. Identifying optimal cleaning cycles for heat exchangers subject to fouling and ageing. Appl Energy. 2012;89:60–6. https://doi.org/10.1016/j.apenergy.2011.01.063.
115. Diaby AL, Miklavcic SJ, Addai-Mensah J. Optimization of scheduled cleaning of fouled heat exchanger network under ageing using genetic algorithm. Chem Eng Res Des. 2016;113:223–40. https://doi.org/10.1016/j.cherd.2016.07.013.
116. Di Pretoro A, D'Iglio F, Manenti F. Optimal cleaning cycle scheduling under uncertain conditions: a flexibility analysis on heat exchanger fouling. Processes. 2021;9:1–18.
117. Al Ismaili R, Lee MW, Wilson DI, Vassiliadis VS. Optimisation of heat exchanger network cleaning schedules: incorporating uncertainty in fouling and cleaning model parameters. Comput Chem Eng. 2019;121:409–21. https://doi.org/10.1016/j.compchemeng.2018.11.009.
118. Hasson D. Rate of decrease of heat transfer due to scale deposition. Dechema-Monogr. 1962;47:233–52.
119. Hasson D, Avriel M, Resnick W, Rozenman T, Windreich S. Mechaniism of calcium carbonate heat-transfer surfaces. Ind Eng Chem Res. 1968;7:59–65.
120. Bansal B, Chen XD, Müller-Steinhagen H. Analysis of "classical" deposition rate law for crystallisation fouling. Chem Eng Process Process Intensif. 2008;47:1201–10.
121. Nikoo AH, Malayeri MR. Incorporation of surface energy properties into general crystallization fouling model for heat transfer surfaces. Chem Eng Sci. 2020;215:115461. https://doi.org/10.1016/j.ces.2019.115461.
122. Bohnet M. Fouling of heat transfer surfaces. Chem Eng Technol. 1987;10:113–25.
123. Segev R, Hasson D, Reegen S. Rigorous modeling of the kinetics of calcium carbonate deposit formation. AIChE J. 2012;58:1222–9.
124. Yang M, Young A, Niyetkaliyev A, Crittenden B. Modelling fouling induction periods. Int J Therm Sci. 2012;51:175–83. https://doi.org/10.1016/j.ijthermalsci.2011.08.008.
125. Briançon S, Colson D, Klein JP. Modelling of crystalline layer growth using kinetic data obtained from suspension crystallization. Chem Eng J. 1998;70:55–64.
126. Jamialahmadi M, Müller-Steinhagen H. Heat exchanger fouling and cleaning in the dihydrate process for the production of phosphoric acid. Chem Eng Res Des. 2007;85:245–55.
127. Esawy M, Malayeri MR. Modeling of $CaSO_4$ crystallization fouling of finned tubes during nucleate pool boiling. Chem Eng Res Des. 2017;118:51–60. https://doi.org/10.1016/j.cherd.2016.11.030.
128. Babuška I, Silva RS, Actor J. Break-off model for $CaCO_3$ fouling in heat exchangers. Int J Heat Mass Transf. 2018;116:104–14.
129. Kapustenko PO, Klemeš JJ, Matsegora OI, Arsenyev PY, Arsenyeva OP. Accounting for local thermal and hydraulic parameters of water fouling development in plate heat exchanger. Energy. 2019;174:1049–59.
130. Souza ARC, Costa ALH. Modeling and simulation of cooling water systems subjected to fouling. Chem Eng Res Des. 2019;141:15–31. https://doi.org/10.1016/j.cherd.2018.09.012.
131. Bobič M, Gjerek B, Golobič I, Bajsić I. Dynamic behaviour of a plate heat exchanger: influence of temperature disturbances and flow configurations. Int J Heat Mass Transf. 2020;163:66.
132. Guelpa E, Verda V. Automatic fouling detection in district heating substations: Methodology and tests. Appl Energy. 2020;258:114059. https://doi.org/10.1016/j.apenergy.2019.114059.
133. Davoudi E, Vaferi B. Applying artificial neural networks for systematic estimation of degree of fouling in heat exchangers. Chem Eng Res Des. 2018;130:138–53. https://doi.org/10.1016/j.cherd.2017.12.017.
134. Aguel S, Meddeb Z, Jeday MR. Parametric study and modeling of cross-flow heat exchanger fouling in phosphoric acid concentration plant using artificial neural network. J Process Control. 2019;84:133–45.
135. Sundar S, Rajagopal MC, Zhao H, Kuntumalla G, Meng Y, Chang HC, et al. Fouling modeling and prediction approach for heat exchangers using deep learning. Int J Heat Mass. 2020;159:66.
136. Benyekhlef A, Mohammedi B, Hassani D, Hanini S. Application of artificial neural network (ANN-MLP) for the prediction of fouling resistance in heat exchanger to MgO-water and CuO-water nanofluids. Water Sci Technol. 2021;84:538–51.
137. Sholahudin Rohman F, Muhammad D, Sudibyo, Nazri Murat M, Azmi A. Application of feed forward neural network for fouling thickness estimation in low density polyethylene tubular reactor. Mater Today Proc. 2022;63:S95–100. https://doi.org/10.1016/j.matpr.2022.02.037
138. Brahim F, Augustin W, Bohnet M. Numerical simulation of the fouling on structured heat transfer surfaces (fouling). ECI Conf Heat Exch Fouling Clean Fundam Appl. 2003;RP1:121–9.
139. Brahim F, Augustin W, Bohnet M. Numerical simulation of the fouling process. Int J Therm Sci. 2003;42:323–34.

140. Walker P, Sheikholeslami R. Assessment of the effect of velocity and residence time in $CaSO_4$ precipitating flow reaction. Chem Eng Sci. 2003;58:3807–16.
141. Xiao J, Li Z, Han J, Pan F, Woo MW, Chen XD. A systematic investigation of the fouling induction phenomena with artificial crystal structures and distributions. Chem Eng Sci. 2017;168:137–55. https://doi.org/10.1016/j.ces.2017.04.043.
142. Yang J. Computational fluid dynamics studies on the induction period of crude oil fouling in a heat exchanger tube. Int J Heat Mass Transf. 2020;159:120129. https://doi.org/10.1016/j.ijheatmasstransfer.2020.120129.
143. Zhang F, Xiao J, Chen XD. Towards predictive modeling of crystallization fouling: a pseudo-dynamic approach. Food Bioprod Process. 2015;93:188–96. https://doi.org/10.1016/j.fbp.2014.10.017.
144. Ojaniemi U, Pättikangas T, Jäsberg A, Puhakka E, Koponen A. Computational fluid dynamics simulation of fouling of plate heat exchanger by phosphate calcium. Heat Transf Eng. 2021. https://doi.org/10.1080/01457632.2021.1963551.
145. Daniali OA, Toghraie D, Eftekhari SA. Thermo-hydraulic and economic optimization of Iranol refinery oil heat exchanger with Copper oxide nanoparticles using MOMBO. Phys A Stat Mech Appl. 2020;540:123010. https://doi.org/10.1016/j.physa.2019.123010.
146. Caputo AC, Pelagagge M, Salini P. Joint economic optimization of heat exchanger design and maintenance policy. Appl Therm Eng. 2011;31:1381–92.
147. Ibrahim H. Fouling in heat exchangers. MATLAB A Fundam tool Sci Comput Eng Appl. 2012;3:57–96.
148. Elwerfalli A, Alsadaie S, Mujtaba IM. Estimation of shutdown schedule to remove fouling layers of heat exchangers using risk-based inspection (RBI). Processes. 2021;66:1–11.
149. Zhi-ming X, Zhong-bin Z, Shan-rang Y. Costs due to utility fouling in China; 2016.
150. Awad M. Fouling of heat transfer surfaces; 2021;
151. ESDU. Heat exchanger fouling in the pre-heat train of a crude oil distillation unit; 2005.
152. Casanueva-Robles T, Bott TR. The environmental effect of heat exchanger fouling: a case study. In: Proceedings of the 6th international conference heat exchange fouling cleaning, challenges opportunities RP2; 2005. p. 5–10.